



Role of Bmal1 in mediating the cholinergic system to regulate the behavioral rhythm of nocturnal marine molluscs



Xiaolong Gao^{a,b}, Mo Zhang^{a,b}, Mingxin Lyu^{a,b}, Shihui Lin^{a,b}, Xuan Luo^{a,b}, Weiwei You^{a,b}, Caihuan Ke^{a,b,*}

^aState Key Laboratory of Marine Environmental Science, College of Ocean and Earth Sciences, Xiamen University, Xiamen 361102, China

^bFujian Key Laboratory of Genetics and Breeding of Marine Organisms, Xiamen University, Xiamen, China

ARTICLE INFO

Article history:

Received 13 February 2022

Received in revised form 17 May 2022

Accepted 19 May 2022

Available online 23 May 2022

Keywords:

Haliotis discus hannai

Movement behaviour

Cholinergic system

AchE inhibitor

Bmal1

ABSTRACT

The circadian rhythm is one of the most general and important rhythms in biological organisms. In this study, continuous 24-h video recordings showed that the cumulative movement distance and duration of the abalone, *Haliotis discus hannai*, reached their maximum values between 20:00–00:00, but both were significantly lower between 08:00–12:00 than at any other time of day or night ($P < 0.05$). To investigate the causes of these diel differences in abalone movement behavior, their cerebral ganglia were harvested at 00:00 (group D) and 12:00 (group L) to screen for differentially expressed proteins using tandem mass tagging (TMT) quantitative proteomics. Seventy-five significantly different proteins were identified in group D vs. group L. The differences in acetylcholinesterase (AChE) expression levels between day- and nighttime and the key role in the cholinergic nervous system received particular attention during the investigation. A cosine rhythm analysis found that the concentration of acetylcholine (ACh) and the expression levels of AChE tended to be low during the day and high at night, and high during the day and low at night, respectively. However, the rhythmicity of the diel expression levels of acetylcholine receptor (nAChR) appeared to be insignificant ($P > 0.05$). Following the injection of three different concentrations of neostigmine methylsulfate, as an AChE inhibitor, the concentration of ACh in the hemolymph, and the expression levels of nAChR in the cerebral ganglia increased significantly ($P < 0.05$). Four hours after drug injection, the cumulative movement distance and duration of abalones were significantly higher than those in the uninjected control group, and the group injected with saline ($P < 0.05$). The expression levels of the core diurnal clock Bmal1 over a 24-h period also tended to be high during the day and low at night. First, a co-immunoprecipitation assay demonstrated the binding between Bmal1 and AChE or nAChR. A dual-luciferase gene test and electrophoretic mobility shift assay showed that Bmal1 bound to the promoter regions of AChE and nAChR. Twenty-four hours after silencing the Bmal1 gene, the expression levels of AChE and nAChR decreased significantly compared to those of the dsEGFP and PBS control groups, further showing that Bmal1 mediates the cholinergic system to regulate the behavioral rhythm of abalone. These findings shed light on the endocrine mechanism regulating the rhythmic behavior of abalone, and provide a reference for understanding the life history adaptation strategies of nocturnal organisms and the proliferation and protection of bottom dwelling economically important organisms.

© 2022 The Author(s). Published by Elsevier B.V. on behalf of Research Network of Computational and Structural Biotechnology. This is an open access article under the CC BY-NC-ND license (<http://creativecommons.org/licenses/by-nc-nd/4.0/>).

1. Introduction

The biological clock is an internal auto-timing mechanism which has evolved after prolonged adaptation to cyclical changes in light, temperature, and other environmental factors (Reppert and Steven, 2002). The Earth's rotation causes environmental factors (including light) to change cyclically over an approximately

24 h cycle, which is mirrored in the circadian rhythms of living organisms. Given the evolutionary history of organisms' adaptation to the Earth's cyclic environment, the biological clock is one of their most pervasive basic characteristics. From single-celled cyanobacteria to complex multicellular fungi, plants, animals, and even human beings, almost all organisms show intense circadian rhythms, and the circadian cycle of 24 h is widely present in cells and organs at all levels from the molecular to the biochemical, and is mirrored in the physiology and behavior of living organisms [50,21]; Ito and Tomioka., 2016). There are slight differences in the

* Corresponding author.

E-mail address: chke@xmu.edu.cn (C. Ke).

core circadian clock genes of eukaryotes, but the circadian clock shares the same regulatory mechanism, namely a transcriptional activation–translation–negative feedback loop [31,27]. In the circadian clock regulatory loop, *Bmal1* and *Clock* are positive components and the encoded proteins Bmal1 and Clock can heterodimerize and bind to the promoter region E-box (CACGTG) or E'-box (CACGTT) of gene sequences, which in turn boosts the transcription of downstream genes. Bmal1 is a member of the bHLH-PAS transcription factor family and conserved domains such as bHLH, PAS-A, and PAS-B are contained in its amino acid sequence. bHLH is the region where DNA binding and dimerization occur, and the formation of dimers often requires the interaction of bHLH and PAS or leucine zipper. PAS is a domain for protein interaction and signal transduction, and most of the bHLH-PAS transcription factor family members have two PAS motifs connected in series: PASA and PASB. Both PAS domains are critical to the formation of dimers and the biological activity of the transcription complex [33,51].

The correlation between the biological clock and metabolic regulation has been extensively investigated, and any disruption or interruption of the circadian rhythm may lead to abnormal glucose and lipid metabolism, diminished immune function, and even anxiety, irritability, and other emotional disorders [3,54]. Endocrine hormones such as melatonin, cortisol, leptin, and ghrelin, which are closely associated with sleep and rhythmic behavior, can directly regulate metabolic processes [40]. Very weak red light at night can lead to a decrease in melatonin sensitivity, thereby disrupting endocrine and metabolic activity rhythms (Dauchy et al., 2015). *Fibroblast growth factor 21* in the suprachiasmatic nuclei, regulates the level of glucocorticoids, changes rhythmic behavior, and adapts cells to starvation environments (Bookout et al., 2013). The expression of glucocorticoid receptor is negatively correlated with the biological clock gene *Clock/Bmal1*, and its transcriptional activity is regulated by the biological clock [25]. Overexpression or disruption of *ecdysone-induced protein 75* in *Drosophila melanogaster* causes the disruption of its activity rhythm and molecular oscillation; it controls the *Clock* gene and may further impact the output route of the biological clock [41].

The cholinergic nervous system forms a critical component of an animal's nervous system and is an important part of the neuroimmune regulatory network. It is largely composed of neurons and uses acetylcholine (ACh) as a neurotransmitter. The normal regulation of physiology is conditional upon the structural integrity of the cholinergic nervous system. At the molecular level, a complete cholinergic signaling pathway consists of ACh, choline acetyltransferase, vesicular acetylcholine transporter, acetylcholinesterase (AChE), choline transporter, and acetylcholine receptor (AChR). Choline acetyltransferase and AChE are ACh metabolic enzymes; the former dominates the synthesis of ACh from choline and acetyl-CoA, while the latter catalyzes the hydrolysis of ACh into choline and acetic acid [5,1]. The choline transporter on the membranes of presynaptic neurons reabsorbs choline in the synaptic cleft, and the choline transporter in neuronal vesicles can enrich the cytoplasmic ACh in vesicles. The vesicular acetylcholine transporter does not only facilitate quantal transmitter packing, but in *Drosophila* also plays a role in glial differentiation, cognitive performance, and locomotion [12,59]. ACh relies on AChR to play its part. After the completion of synaptic transmission, ACh is hydrolyzed into choline and acetic acid by AChE in the synaptic cleft, which in turn halts the transduction of nerve signals [14]. AChE also plays a significant role in other physiological processes, including embryonic development, cell proliferation, differentiation, cytoskeleton assembly, cell adhesion, and immunity, in addition to classic hydrolysis. Choline acetyltransferase, vesicular acetylcholine transporter, AChE, AChR, and choline transporter all play significant roles in the synthesis and release of ACh and cho-

line signal transduction. Abnormal changes in any of these processes preclude the transduction of cholinergic signals, thereby impacting a series of internal physiological activities (Sethuramanujam, 2021; Santos et al., 2007; [18,47].

Haliotis discus hannai is one of the most important mariculture shellfish in China. In 2019, its aquacultural production reached 180,300 tons, accounting for about 90% of the world's total (China Fisheries Yearbook, 2020). As a typical nocturnal creature, its feeding and movement behaviors generally occur at night, while it scarcely moves during the day [19]. Nocturnal activity generally protects some animals from predators, such as abalone, which move slowly and depend solely on the passive protection afforded by a shell. It is a result of ongoing adaptation to the environment, and provides basic guarantees for successful reproduction. The rhythmic reciprocating response to an approximately 24-h cycle makes abalone a good model for the study of the origin and evolution of behavioral rhythms in nocturnal marine organisms. It is also a preferred subject for investigations into the molecular regulatory mechanisms of the diurnal clock. However, there are no reports of the molecular mechanisms governing the rhythmic behavior of abalone thus far. Even though their molecular biological clock mechanisms are well-known, little is known about how time signals are transmitted from the biological clock to regulate physiology and behavior. This study therefore set out to use video surveillance techniques to quantify the movement behavior parameters of abalone, and then screen for the key proteins that are differentially expressed during the day and at night. Tandem mass tagging (TMT) high-throughput proteomics was used to reveal the interactions between core diurnal clock genes by functional interpretation of the temporal and spatial expressions of differential proteins, and ultimately identify the endogenous regulatory mechanism of the rhythmic behavior of abalone and so enable the light conditions used in aquacultural production to be optimized.

2. Materials and methods

2.1. Source and acclimation of experimental abalones

Artificially hatched experimental abalones (shell length 7.02 ± 0.76 cm, body weight 65.33 ± 3.82 g) from a single batch were purchased from the Fuda Abalone Aquafarm (Jinjiang, Fujian, China). Prior to the experiment, the abalones were placed into four culture tanks (0.8 m long \times 0.4 m wide \times 0.4 m high) and kept at a light cycle of 12L:12D to acclimate for 15 days. The seawater was continuously aerated and changed once a day. The water conditions were kept at: 20°C; salinity 30 ± 1 ; pH 8.0; and dissolved oxygen concentration > 6.5 mg/L. The culture water was natural seawater and was used after sedimentation and sand filtration. Fresh *Gracilaria lemaneiformis* was fed every day at 3% of the wet weight of abalone, to ensure that the abalones reached satiation.

2.2. Experimental unit

The behavior monitoring unit was composed of two parts: an experimental breeding section and a video surveillance section housed in a round polyethylene tank with a diameter of 1.2 m and height 0.35 m. The entire unit was covered with a cloth to completely eliminate external light and lit with a built-in LED to control the lighting conditions. The movement behavior of the abalones was recorded using an infrared camera (HIKVISION, Hangzhou, China) located above the center of the surveillance section. The camera's field of vision extended to the outer bottom edge of the tank. The light intensity at the bottom part of the tank was about 31.64 ± 8.41 lx. The experimental videos were made and

stored inside the video surveillance unit. The light cycle was controlled using a clock controller. The total recording time was 24 h with 5-s time intervals, and the video format was AVI with a resolution of 680×480 pixels at 10 fps.

2.3. Experimental design

To ascertain the movement behavior characteristics of abalone during the day and at night, 32 abalones were selected at random. Groups of four were placed in an experimental unit to monitor their cumulative movement distance and duration, with eight repeats per group. The experimental cycle was set at 24 h, and the light source was turned on and off at 06:00 am and 18:00 pm, respectively. A continuous video was recorded of their movement behavior. After the light source was turned off, the seaweed *Gracilaria lemaneiformis* was fed once at 3% of the wet weight of abalones. The experimental unit comprised a recirculating aquaculture system, and the seawater was replenished once every three days to offset losses due to evaporation. Following the experiment, the abalones were transferred to their original cages for acclimation but were not reused. Labels were fixed to the shells to differentiate between individuals during the experiments, and the videos were analyzed using XT Ethovision 9.0 (Noldus Information Technology, Wageningen, Netherlands).

To shed light on the mechanism regulating differences in the movement behavior of abalones by day and night, two groups of 18 abalones were selected at random and one group was dissected at 12:00 am (group L) and the other at 0:00 pm (group D). The cerebral ganglia were collected and transferred to three 1.5 mL centrifuge tubes. Given the tiny size of the cerebral ganglia, each tube contained a mixed sample of the ganglia of six abalones. The tubes were immediately stored in liquid nitrogen for TMT proteomics analysis. Next, the differential proteins AchE and AchR, forming part of the cholinergic system, were subjected to gene cloning and phylogenetic analysis based on the findings of the proteomics analysis. Then, 45 abalones were selected at random from the holding cages (kept at 12L:12D); six were taken at successive time points: 08:00 (ZT0), 12:00 (ZT4), 16:00 (ZT8), 20:00 (ZT12), 00:00 (ZT16), 04:00 (ZT20), and 08:00 (ZT24) and the blood sinusoids were cut off. The blood taken was centrifuged at 3000 g for 15 min in a 1.5 mL centrifuge tube, and then immediately stored in liquid nitrogen for the later determination of ACh concentrations. The foot muscles, cerebral ganglia, gills, intestines, mantles, hepatopancreas, and cephalic tentacles were collected and used to determine the expression levels of *AchE* and *nAChR* in the seven different tissues, at the seven different time points. The cerebral ganglia were used to determine the corresponding expression levels of these genes. The cerebral tissue of the remaining three abalones was collected and transferred to 4% paraformaldehyde stationary solution, and the specific sites on the cerebral ganglia at which AchE and nAChR were expressed were located using *in situ* hybridization. To avoid interference from the white light source during the nighttime experiments, a special long-wavelength red light (wavelength = 640 nm) was used as the light source during sampling processing at night. After the samples were collected from the cages, the abalone's cerebral tissues were dissected in order to collect cerebral ganglia. To further identify whether the cholinergic system may be involved in the regulation of cyclical movement behavior, 60 more abalones were selected at random and injected with different concentrations of AchE inhibitor and observed by video for 24 h (see section 2.4.6). The 24 h video recordings were analyzed to quantify their movement behavior characteristics, and the expression levels of *AchE* and *nAChR* and the changes in concentration of ACh were determined. In the final step (see section 2.4.8), to ascertain possible internal correlations between the rhythmic expression of *AchE* and *nAChR*

and the core diurnal clock gene *Bmal1*, the diurnal expression of *Bmal1* was determined using fluorescent quantitative PCR. The promoter sequences for AchE and nAChR were obtained, and direct regulation of AchE and nAChR by *Bmal1* was validated using a dual-luciferase reporter gene assay and electrophoretic mobility shift assay (EMSA).

2.4. Assay of samples

2.4.1. TMT quantitative proteomic identification of differentially expressed proteins

Samples were minced individually with liquid nitrogen and lysed in lysis buffer containing 100 mM NH_4HCO_3 (pH = 8), 6 M urea, and 0.2% SDS, followed by 5 min of ultrasonication on ice. The lysate was centrifuged at 12,000 g for 15 min at 4 °C and the supernatant was transferred to a clean tube. Protein concentration was determined using a Bradford protein assay. The supernatant from each sample containing precisely 0.1 mg of protein was digested with Trypsin Gold (Promega, USA) at 1:50 enzyme-to-substrate ratio. After 16 h of digestion at 37 °C, peptides were desalted with C18 cartridge to remove the high urea. The desalted peptides were dried via vacuum centrifugation and labeled with TMT6/10-plex reagents (TMT6/10plex™ Isobaric Label Reagent Set, Thermo Fisher) following the manufacturer's instructions. TMT-labeled peptide mix was fractionated using a C18 column (Waters BEH C18 4.6 \times 250 mm, 5 μm) on a Rigol L3000 HPLC operating at 1 mL/min. The column oven was set to 50 °C. The eluates were monitored at UV level of 214 nm, collected for a tube per minute, and finally merged into 10 fractions. All fractions were dried under vacuum and reconstituted in 0.1% (v/v) formic acid (FA) for subsequent analyses. Shotgun proteomics analyses were performed using an EASY-nLCTM 1200 UHPLC system (Thermo Fisher) coupled with an Orbitrap Q Exactive HF-X mass spectrometer (Thermo Fisher) operated in the data-dependent acquisition (DDA) mode. Q Exactive HF-X mass spectrometer was operated in positive polarity mode with spray voltage of 2.3 kV and capillary temperature of 320 °C. The 40 most abundant precursor ions from a full MS scan were selected for fragmentation using higher energy collisional dissociation (HCD) at a resolution of 15,000 (at 200 m/z) with an AGC target value of 1×10^5 , a maximum ion injection time of 45 ms, a normalized collision energy of 32%, an intensity threshold of 8.3×10^3 , and a dynamic exclusion parameter of 20 s.

The resulting spectra from each fraction were separately searched against the X101SC19060472-Z01-Hdh. changID. fasta and Hdh. Swissprot_Annotation. xls databases using the Proteome Discoverer 2.2 search engine (PD 2.2, Thermo Fisher Scientific, Waltham, MA, USA). The searched parameters used were: a mass tolerance of 10 ppm for precursor ion scans; and a mass tolerance of 0.02 Da for the product ion scans. Regarding protein identification, proteins with at least one unique peptide were identified with a false discovery rate of <1.0% at the peptide and protein levels. Proteins containing similar peptides which could not be distinguished based on MS/MS analysis were categorized into separate protein groups. Reporter Quantification (TMT) was used for TMT quantification. The protein quantification results were analyzed statistically using Mann-Whitney tests, with significance ratios set at $P < 0.05$ and FC in the range 1.5–0.67, to screen the differentially expressed proteins (DEPs). Gene Ontology (GO) and InterPro (IPR) analyses were conducted using the Interproscan-5 program against non-redundant protein databases (including Pfam, PRINTS, ProDom, SMART, ProSiteProfiles, PANTHER), and the Kyoto Encyclopedia of Genes and Genomes (KEGG) database was used to analyze the protein families and pathways. An enrichment pipeline was used to perform the enrichment analyses of GO, IPR and KEGG.

2.4.2. Cloning and phylogenetic analyses of AchE and nAchR

The total RNA of the cerebral ganglia was extracted using TRIzol (Invitrogen, USA) and 1% agarose gel electrophoresis (AGE) was used to detect the integrity of the RNA. The concentration and purity of the RNA were detected using a spectrophotometer. cDNA was synthesized using a Prime Script RT reagent kit with a gDNA eraser kit (TaKaRa, Japan). RACE-Ready cDNA was synthesized using a SmartTM RACE cDNA amplification kit (TaKaRa, Japan). Retrieving the proteomics and the genome data of *H. discus hannai* allowed discovery of the preliminarily gene sequences of the candidate AchE and nAchR. Primers were designed for PCR amplification of the above candidate sequence segments, in order to validate their open reading frame (ORF) regions (Table 1). The PCR amplification system comprised 25 µL of 2 × ExTaq Mix (TaKaRa, Japan). Each ORF-F/R primer comprised 1 µL. The cDNA template comprised 2 µL ddH₂O, replenished to 50 µL. The PCR amplification conditions were: 94°C for 4 min; 33 cycles (94°C 30 s, 58°C 30 s, 72°C 60 s, 72°C 7 min). PCR products were detected using agarose gel electrophoresis and purified and recovered using a DNA gel recovery kit. The purified segments were ligated to the pEasy-T1 vector and transferred to Trans-T1 competent cells using the 42 °C heat shock method. Finally, a single clone was screened out and sent to Sangon Biotech Co., Ltd. (Shanghai, China) for sequencing to obtain the ORF region sequence. RACE primers were designed according to the ORF region sequences (Table 1), using synthesized RACE-Ready-cDNA as a template. 5'-RACE and 3'-RACE PCR amplification was conducted using touchdown PCR, as follows: 94°C 30 s; 72°C 3 min, 5 cycles; 94°C 30 s, 70°C 30 s, 72°C 5 min, 5 cycles; 94°C 30 s, 70°C 30 s, 72°C 3 min, 25 cycles; with a final extension at 72°C for 10 min. After the amplification, molecular cloning was per-

formed, and a single clone from Sangon Biotech was screened out for sequencing purposes. 5' and 3'-sequences were successfully obtained and then spliced using DNASTar, until a full-length cDNA sequence was obtained. The AchE and nAchR amino acid sequences of *H. discus hannai* and other animals were used to construct a phylogenetic analysis. The signal peptide sequence and functional domain of these proteins were predicted using SMART 4.0 (<https://smart.embl-heidelberg.de/>). The relative molecular mass and theoretical isoelectric points of AchE and nAchR were calculated using ProtParam (<https://au.expasy.org/tools/protparam.html>), included in the ExpASY online software. The phylogenetic tree was constructed using the Neighbor-Joining (NJ) technique included in MEGA 7.0, with the bootstrap set to 1000. The amino acid sequences of AchE and nAchR were compared with the different species on DNAMAN.

2.4.3. Assay of the expression levels of AchE, nAchR, and Bmal1 in different tissues during the day and night

The samples from each tissue were stored in liquid nitrogen, ground, and then quickly mixed with 1 mL TRIzol (Invitrogen, USA) to extract the total RNA. The quality and concentration of RNA were assessed using a NanoDrop 1000 (Thermo Fisher Scientific, Waltham, MA, USA). The indexes of biotic integrity (IBIs) of all the extracted RNA samples were ≥ 9.4, with an RNA ratio (28S/18S) ≥ 1.8. Total RNA was extracted by removing the residual DNA from the samples using RQ1 RNase-Free DNase (TaKaRa, Japan) and the RNA was then reversely transcribed to cDNA using M-MLV reverse transcriptase (Promega, USA). Real-time quantitative PCR tests were performed using a SYBR® Premix Ex Taq™ II kit

Table 1
Gene specific primers used in this study.

Gene	Sequence (5'-3')	GenBank accession	Usage
AchE	F: CGGAAACTCCACTGATTCATC R: TCCGCTTGGGCAAGCATCG	OK509160	Real-time RT PCR
nAchR	F: GCCAAACTCCAGAATGAC R: CAGAACCCGGATTGGCAGT	OK424911	Real-time RT PCR
Bmal1	F: TTGGCACCCTGCAGTTTGTC R: GACATTGAGGGACAAACG	MN822015	Real-time RT PCR
18S	F: TTCCAGTAAGCGTCAGTCATC R: CGAGGGTCTCAATAAACCATTC	AY319437.1	Real-time RT PCR
AchE	F: GGTGGCCAGGATGGCTCAC R: CAAGAGGGTTGGGGTTGTTG		CDS amplification
nAchR	F: TCCCTTATACTCTGACAGTTTGAT R: AGGTCTCTGGTGGCTGTTA		CDS amplification
AchE	F1: CGAGATTATCTCGACTTCCGCTGG F2: GATACAGTAGCGAGGAGTGGACCTGAG R1: CGATACTCTGATGACAGGAGTTGGGCAT R2: GTGTTCCAGGGTCTGTAGGCA		3' RACE 5' RACE
nAchR	F1: GACAGTGCAGCATCGATTATTGAAGATTGG F2: GTCGCCATGGTGTAGATCGGCT R1: ACGTATAACTTGTCCGATTCATCCCCAC R2: GGGACAATCCGATGCCAGCTT		3' RACE 5' RACE
AchE	GW1: GACGCTTCGACCCATCG GW2: TTCGCAATCGGGCTACCCG GW3: TTTCATATTTTCGCTCTCATTGAG		Promoter verification
nAchR	GW1: ATGCCCGAACGACCTCTTGTC GW2: ACCTGATTTAACATTCTTGGGT GW3: TTTTATGAGTTCAACATTTTTTCAAGAT		Promoter verification
Bmal1	F: <u>TACCACGACTCGCTATACGGAACAGAACCCGACACCAGAT</u> R: <u>TACCACGACTCGCTATACGGCTCTCGACACCACTAACTTC</u>		dsRNA synthesis
EGFP	F: <u>TACCACGACTCGCTATACGGGACCCGACA</u> CGGAACAGTT R: <u>TACCACGACTCGCTATACGGCTTGCACA</u> AATCGTCGCC		dsRNA synthesis
Bmal1	F: CGAACGTAGACCGTTCCGGAGGC R: GCAACTCATATCCGCCGACACTACCT		EMSA

Note: F: Forward primer; R: Reverse primer. GW1 and GW2: primary PCR primer; GW3: nested PCR primer.

(Tli RNaseH Plus) (TaKaRa, Japan) and a TaKaRa Thermal Cycler Dice™ Real Time System TP800 instrument. A 20 µL reaction system was used in the PCR tubes comprising: 10 µL of SYBR® Premix Ex Taq TM II, 0.5 µL of forward primer (10 µM), 0.5 µL of reverse primer (10 µM), 1 µL of DNA template, and 8 µL of dH₂O.

The primer sequence (Table 1) for fluorescent quantitative analysis was designed according to the sequence information for the cloned AchE, nAChR, and Bmal1 using primer3 (v0.4.0; <https://bioinfo.ut.ee/primer3-0.4.0/primer3/>). The sample was evenly mixed in a PCR tube and then placed onto a PCR plate (Roche Diagnostics, Indianapolis, IN, USA). PCR amplification was performed after transient centrifugation. The reaction conditions were as follows: initial denaturation at 94 °C for 30 s. The cycling conditions were as follows: 94 °C for 5 s and 60 °C for 30 s, 40 cycles in total. Melting curve analysis was carried out at the end of the experiment. PCR analyses were repeated three times for each RNA sample and gene. Target gene mRNA levels were calibrated using the real-time PCR Ct (2^{-ΔΔCt}) relative quantitative method, where the reference gene 18S served as the quantitative standard.

2.4.4. Ach concentration determination and cosine rhythm analysis

The moisture on the surface of abalones was absorbed using blotting paper. The surface of the feet was sterilized with alcohol, and the blood sinusoids were cut off with a sterilized scalpel, collecting blood using a pipette. The blood samples were transferred to a centrifuge tube, kept at room temperature for 20 min, and centrifuged at 3000 g for 10 min. The supernatant was then collected. The samples were analyzed using an ELISA kit (Code: CS-00E985215) supplied by Shanghai Chuntest Biotechnology Co., Ltd.

The concentration of ACh was determined using the double antibody sandwich method. The kit assay for the ACh level in the sample used purified ACh antibody to coat the microtiter plate wells to produce solid-phase antibodies. The ACh was added to the microwells and then bound to the labeled antibodies detected using labeled horseradish peroxidase (HRP), until an antibody-antigen-enzyme labeled antibody complex was formed. The seals were removed and the liquid discarded. Each microwell was filled with washing fluid and washed five times before 3,3',5,5'-tetramethylbenzidine (TMB) was added for color developing. The TMB first turned blue as it was catalyzed by the HRP, before finally turning yellow under the action of the sulfuric acid solution. The depth of color was positively correlated with the ACh concentration in the samples. The absorbance value (OD) was measured using a microplate reader at 450 nm, and the ACh concentrations in the samples were calculated from standard curves.

2.4.5. In situ hybridization of AchE and nAChR

The samples were first removed from the stationary liquid and then subjected to gradient alcohol dehydration. After wax impregnation and embedding, the samples were sectioned and the sections were placed in xylene for 15 min, absolute ethanol for 5 min, 85% alcohol for 5 min, and finally 75% alcohol for 5 min, and then flushed with DEPC treated water. Samples were then boiled in EDTA antigenic repair solution for 15 min and left to cool naturally before dipping in proteinase K (20 µg/mL), digested at 37 °C for 30 min, and then flushed three times with PBS. Dipped pre-hybridization solutions (50% deionized formamide, 5% 50 × Denhardt's solution, 5% tRNA (20 mg/mL), 15% DEPC water, 10% dextran sulfate, and buffer salt solution) were incubated at 37 °C for 1 h. With the pre-hybridization solution discarded, samples were dipped in the hybridization solution at a concentration of 8 ng/µL with the chosen probes (AchE, antisense probe 5'-GCCAAU GAAAAGCGACCAUUGUUAGCUUA-3', sense probe 5'-CGGUUA CUUUUCCGUGGUAACAAUCGAU-3'; nAChR, antisense probe 5'-UUGCGUGAAGAAUCCACAUAGAGGAGACCGGU-3', sense probe 5'-AACGCACUUCUACGGUGUAUCUCCUCUGGCA-3') and left

overnight in a thermotank at 37 °C. On the next day, the hybridization solution was eluted with saline sodium citrate (SSC), and the sections were coated with DAPI staining solution (2 µg/mL) and incubated in a dark area for 8 min. After washing, the sections were dripped with antifade mounting medium, mounted and observed under an upright fluorescence microscope for image acquisition.

2.4.6. The effects of injection of AchE inhibitor on the expression levels of AchE and nAChR, and ACh concentration and the corresponding movement behavior of abalones

To validate the neuroendocrine regulatory effect of AchE on the periodic movements of abalones, 60 abalones were selected at random and divided into five groups of 12 each. One group was injected with normal saline, and three others were injected with 7.48×10^{-7} mol, 1.50×10^{-6} mol, or 2.99×10^{-6} mol neostigmine methylsulfate (C₁₃H₂₂N₂O₆S, spec: 1 mL: 1 mg, Shanghai Pharmaceuticals Holding Co., Ltd., China) as an AchE inhibitor. The last group formed the control and was not injected. The injections were made into the blood sinus of the foot using a micro-syringe. As revealed in the experiments described in section 2.3, the movement distance and duration of *H. discus hannai* were short between 08:00–12:00. Abalones were therefore observed for 4 h after injection starting at 08:00am. Four abalones were selected each time, and their cumulative movement distance and duration were recorded once every 1 h. After the behavioral experiment, the blood and cerebral ganglion tissues of all abalones in each group were harvested and collected. Three thousand grams of hemolymph from each individual were centrifuged for 10 min and the supernatant was collected and stored in liquid nitrogen for ACh content assay. The cerebral ganglion samples were stored at -80 °C in a refrigerator for measurement of the expression levels of AchE and nAChR.

2.4.7. Validation of the interaction between Bmal1 and AchE or nAChR

Cell culture and transfection: HEK293T cells were cultured normally in 10% FBS + DMEM medium. When the cell density reached 90% or higher, it was rinsed with PBS, the supernatant was discarded, and 0.25% trypsin and 10% FBS + DMEM culture solutions were added sequentially, and the sample was placed into a culture dish. After all of the cells had exfoliated, the cells were placed onto a counting plate and counted. The cell culture solution in the 6-cm culture dish was substituted with Opti-MEM in new tubes and labeled either A (those with added Opti-MEM + 5 µg plasmid (2.5 µg each of Bmal1-HA and AchE-FLAG or Bmal1-HA and nAChR-FLAG) or B (those with added Opti-MEM + 10 µL Lipofectamine 3000), mixed, and left to stand for 20 min for fluorescence observation the next day.

Co-immunoprecipitation: the cell samples co-transfected with plasmid for 48 h were collected and used in an immunoprecipitation experiment. Cells were washed twice with PBS and pre-cooled RIPA Buffer was added to scrape the cells off the culture dish. One hundred microliters of Protein A agarose beads were added per 1 mL of total protein, centrifuged and the supernatant was then transferred to a new centrifuge tube. The Protein A beads were removed and the protein concentration was determined. Rabbit antibody was added to 500 µL total protein, incubated at room temperature for 2 h, and 100 µL Protein A agarose beads were then added to capture the antigen-antibody complex. After incubation at room temperature for 1 h, the agarose beads-antigen-antibody complex was collected, rinsed with RIPA buffer three times, after which the agarose beads-antigen-antibody complex was suspended using loading buffer. The remaining agarose beads were collected by electrophoresis and the cells were scraped into EBC lysis buffer. The cell suspension was transferred to a microcentrifuge tube and centrifuged for 15 min. The supernatant (500 µL) was collected, and HA/FLAG antibody (10 µg) and protein

A-Sepharose suspension (100 μ L) were added sequentially, and the protein A-Sepharose mixture was rinsed five times with NETN. Finally, the sample was added to SDS-PAGE gradients and electrophoresed at a constant current of 10 mA overnight.

Western blot testing: the protein samples subjected to immunoprecipitation were separated using 10% SDS-PAGE and the gels, filter papers and PVDF membranes were then soaked in transfer buffer for 10 min for semi-dry electrophoresis. The position of the marker band was marked, and the transfer film was blocked using blocking buffer for 2 h, washed three times with $1 \times$ TBST, and incubated with primary antibody overnight. On the next day, a diluted secondary antibody was added for 2 h, washed five times with $1 \times$ TBST, subjected to chemiluminescence detection and X-ray film exposure, and finally developed and fixed prior to photography using a gel imaging analysis system.

2.4.8. *Bmal1* binds to the promoter sequence of *AchE* and *nAChR*

In the course of the experiment, *AchE* and *nAChR* promoter sequences were cloned using a Universal Genome Walker 2.0 Kit (Clontech, USA). Five DNA libraries were created using the completed genomic data and labeled as HD-1, HD-2, DL-3, DL-4, and PvuII Positive Control. Each gene was designed with two pairs of specific primers: two for primary PCR (GW1 and GW2) and the other for nested PCR (GW3) (Table 1).

NC + *AchE*-WT, NC + *nAChR*-WT luciferase vector, *Bmal1* overexpression + *AchE*-WT, *Bmal1* overexpression + *nAChR*-WT luciferase vector, NC + *AchE*-MUT, NC + *nAChR*-MUT luciferase vector, *Bmal1* overexpression + *AchE*-MUT, and *Bmal1* overexpression + *nAChR*-MUT luciferase vector were co-transfected using a Dual-Luciferase Reporter Assay System (Promega, Madison, WI, USA) in order to ascertain the effects of *Bmal1* on *AchE*-WT, *AchE*-MUT, *nAChR*-WT, and *nAChR*-MUT in HEK293T cells. The 293 T cells were seeded into a 24-well plate at a confluence of 30–50%. The target and control plasmids were transfected 24 h later. After 48 h of transfection, the medium was discarded and rinsed once with $1 \times$ PBS. The remaining PBS was absorbed and diluted $1 \times$ PLB (Passive Lysis Buffer) was added to each well for lysis and shaken at normal temperature for 15 min. A total of 20 μ L of pre-mixed Luciferase Assay Reagent II (LAR II), 1 μ L of cell lysate supernatant, and 29 μ L of water were added to each well of an opaque white 96-well plate, and measurements were taken after 2 s. Finally, 20 μ L of pre-mixed Stop & Glo Reagent were immediately added to each well and measurements were taken after 2 s of rest. Results were obtained by dividing the Firefly luciferase by the *Renilla* luciferase data. The mean values were used for graphic representation.

Next, EMSA was used to detect the binding between *Bmal1* protein and *AchE* or *nAChR* gene promoters (binding sites CACGTT or CACGTG). In the first step, recombinant expression of the *Bmal1* protein was performed, and the recombinant *Bmal1* protein was transcribed *in vitro* using the 1-Step Human Coupled IVT Kit (Thermo Scientific, USA). CDS fragments were amplified using *Bmal1*-specific primers (Table 1) with restriction enzyme-cutting sites. The pT7CFE1-Chis Expression Vector and *Bmal1* fragment were subjected to double digests by Bam HI and Not I. The *Bmal1* fragment was linked to the pT7CFE1-Chis expression vector in order to construct the expression plasmid *Bmal1*-pT7CFE1-Chis expression vector. The reactant was prepared at room temperature (HeLa lysate 12.5 μ L, accessory proteins 2.5 μ L, reaction mix 5 μ L, pCFE-*Bmal1* DNA 1 μ g, with nuclease-free water added to achieve a total volume of 25 μ L), added to the centrifuge tube, mixed gently, and reacted at 30 $^{\circ}$ C for 5 h until the recombinant *Bmal1* protein was obtained. The specific detection of recombinant protein was performed using anti-6 \times His rabbit polyclonal antibody and HRP-conjugated goat anti-rabbit IgG (Sangon Biotech, Shanghai, China). In the course of the EMSA experiment, the Lightshift

Chemiluminescent EMSA kit (Thermo Scientific, USA) was used. Based on the promoter sequences for *AchE* and *nAChR*, two single-stranded probes with reverse complement were designed and synthesized, and the 3' end was labeled with biotin. The two labeled single strands with reverse complement were mixed at equal volumes and $10 \times$ PCR buffer was added for even mixing. The samples were incubated at 95 $^{\circ}$ C for 10 min, slowly cooled at room temperature (2 h), and stored at -20° C for future use. To account for the interaction between transcription factors and DNA, a negative control group (binding buffer 2 μ L, purified protein 0 μ L, labeled probe 10 pmol, with nuclease-free water added to achieve a total volume of 10 μ L) and a cold competition control (binding buffer 2 μ L, purified protein 2 μ L, 100 \times unlabeled probe 1 nmol, labeled probe 10 pmol, with nuclease-free water added to achieve a total volume of 10 μ L) were further designed for corroborative evidence in addition to the experimental group (binding buffer 2 μ L, purified protein 2 μ L, labeled probe 10 pmol, with nuclease-free water added to achieve a volume of 10 μ L). Electrophoresis solution consisted of $0.5 \times$ TBE and was used at 4 $^{\circ}$ C and 125 V. A membrane transfer instrument was used to transfer the membrane at a constant current of 5.5 mA/cm² for 20 min. After irradiation with a UV lamp for 10 min, the membrane was cross-linked, transferred into a sealed bag containing blocking solution, shaken for 15 min, and then incubated with 7.5 μ L of streptavidin-HRP conjugate for 30 min. The membrane was taken out after incubation, transferred to a washing solution, rinsed for 5 min, coated with ECL color developing solution, and photographed.

2.4.9. Screening of *Bmal1* interference doses and their effects on the expression levels of *AchE* and *nAChR*

To detect whether the interactions with *Bmal1* would influence the expression of potential target genes, a fragment of *Bmal1* was initially amplified at the T7 junction using the primers *Bmal1*-T7-F and *Bmal1*-T7-R (Table 1), to create a template for the synthesis of double-stranded RNA (ds*Bmal1*). The EGFP fragment was amplified in plasmid pEGFP (Clontech, USA) using the primers EGFP-T7-F and EGFP-T7-R at the T7 junction, and used as a template for the synthesis of double-stranded dsEGFP. ds*Bmal1* and dsEGFP were then synthesized and purified using a Transcript Aid T7 High Yield Transcription Kit (Thermo Scientific, USA). Finally, the concentrations of the RNA double strands were measured using a Nanodrop ND1000 spectrophotometer (Thermo Scientific, USA).

Abalones were randomly divided into three groups: ds*Bmal1* group, dsEGFP group (negative control group), and PBS group (blank control group), with 20 abalones assigned to each group. Double-stranded RNA (ds*Bmal1*/dsEGFP) was diluted in PBS and four injection doses (0.5, 1, 2, and 5 μ g/g body weight) were established. The various doses of ds*Bmal1*, dsEGFP and PBS were injected into the blood sinuses of abalones in the ds*Bmal1*, dsEGFP, and PBS groups, respectively. After 24 h, the cerebral ganglia tissues of five abalones in each injection doses group were subjected to RNA extraction, and the expression levels of *Bmal1* were detected using qPCR. To further identify the regulatory effects of *Bmal1* on *AchE* and *nAChR*, the other 20 abalones were dissected 24 h after injection, the cerebral ganglia were removed, and the expression levels of *AchE* and *nAChR* in the experimental and control groups were measured using qPCR, after determining the interference dose and evaluating the interference outcome.

2.5. Data analysis

Prior to data analysis, Kolmogorov-Smirnov and Levene's tests were used to judge the normal distribution and the homogeneity of variance of the data. The movement behavior parameters of the abalones, the Ach content, the expression levels of *AchE* and

nAChR in the different tissues, the trends in the expression levels of *AchE*, *nAChR*, and the Ach content following the injection of different concentrations of AchE inhibitor were analyzed using One-Way ANOVA combined with Tukey's multiple comparison, in SPSS v18.0. Differences in the cumulative movement distance and duration of abalones in any period following the injection of different concentrations of specific inhibitors were analyzed and compared using two-way ANOVA and Tukey's multiple comparison. The data were presented as means \pm standard deviation (mean \pm SD), with a significance level of $P < 0.05$. The data thus acquired were plotted using Sigmaplot.

Cosine fitting was performed on the data related to Ach concentration and expression levels of AchE and *nAChR* using the Cosinor program package in Matlab, with $Y = M + A \cos(\omega t + \Phi)$ as the calculation model. M (MESO) represents the median value of the fitted cosine curve. A , ω , and Φ represent the amplitude, angular frequency, and peak value of the cosine fitting, respectively. t stands for the diurnal time points around 24 h. Y stands for the Ach concentration and expression levels of corresponding genes measured at each point every 4 h. The values of M , A , and Φ in the cosine fitting curves can then be obtained [32].

3. Results

3.1. Cumulative movement distance and duration of abalones over a 24 h period

Based on uninterrupted 24 h observations, the cumulative distance moved by abalones from 08:00–16:00 was significantly lower than in any other period (Fig. 1a, $P < 0.05$). The cumulative distance moved by abalones reached its maximum between 20:00–00:00, but was not significantly different from that between 16:00–20:00. The cumulative movement duration of abalones between 20:00–00:00 was significantly longer than during any other period. It was significantly shorter between 08:00–12:00 than in any other period (Fig. 1b, $P < 0.05$).

3.2. Identification of differentially expressed proteins

Given the diurnal differences in the movement behavior of abalone, we intended to use mass spectrometry to identify and screen key proteins that may potentially lead to these behavioral changes between day and night. After searching databases against the mass spectrometry data, a series of quality controls such as peptide length distribution, parent ion mass tolerance distribution, unique peptide number distribution, and protein coverage distribution were performed: 405,174 secondary spectra, 40,528 peptides, and 4479 proteins were identified. According to the GO annotation results, most proteins were assigned to the Oxidation-reduction Process term in Biological Processes (236). Regarding the Cellular Component category, up to 181 were assigned to the Membrane term. Regarding the Molecular Function category, up to 740 were assigned to the Protein Binding term (Fig. 2a).

Of the 4479 proteins identified, there were 75 proteins with significant differences, of which 26 significantly increased their expression levels and 49 significantly decreased their expression levels (Fig. 2b). According to the COG class descriptions, secondary metabolites biosynthesis (cytochrome P450 2 J2, peroxidase-like protein 3), lipid transport and metabolism (cholinesterase), signal transduction mechanisms (sarcolemmal calcium-binding protein, calmodulin-4), amino acid transport and metabolism (angiotensin-converting enzyme), carbohydrate transport and metabolism (Beta-1,3-glucan-binding protein) were identified.

Using the KEGG pathway categories as the unit, a hypergeometric test was conducted to discover all of the pathways that were

significantly enriched in the differential proteins, compared to all of the proteins identified. One hundred and fourteen metabolic pathways were enriched in group D vs. group L, in which 11 were significantly enriched, including Metabolism of Xenobiotics by cytochrome P450, phototransduction-fly, and glutathione metabolism (Supplementary Fig. 1). AchE is not only an essential enzyme for the hydrolysis of the neurotransmitter Ach, but also directly impacts changes in the movement behavior of animals, and was therefore considered the focus differential protein in this work.

3.3. Sequence cloning and phylogenetic analysis of AchE and nAChR

The cDNA of AchE has a full length of 2,260 bp (accession number: OK509160), including the 5' non-coding region (76 bp), the 3' non-coding region (387 bp), the ORF (1,797 bp), and the encoded amino acids (599 bp) (Supplementary Fig. 2a). Its amino acid sequence contains a signal peptide (1–23), a carboxylesterase family domain (24–547), an alpha/beta hydrolase fold domain (188–314), and a prolyl oligopeptidase family domain (148–273). It has a molecular weight of 67.45 kDa, a theoretical isoelectric point of 5.69, and a grand average of hydropathicity of -0.256 . The cDNA of *nAChR* has a full length of 2,405 bp (Accession number OK424911), including the 5' non-coding region (117 bp), the 3' non-coding region (743 bp), the ORF (1,545 bp), and the encoded amino acids (515 bp) (Supplementary Fig. 2b). Its amino acid sequence contains a signal peptide (1–23) and five transmembrane domains (5–24, 250–268, 280–299, 312–331, and 474–492), as well as a neurotransmitter-gated ion-channel ligand binding domain (27 ~ 246) and a neurotransmitter-gated ion-channel transmembrane region (253 ~ 491). Its molecular weight is 58.60 kDa, its theoretical isoelectric point is 5.49, and its grand average of hydropathicity is 0.030. According to a homology comparison with the amino acid sequence of other species, the AchE sequence of *H. discus hannai* is conserved, especially in some key functional areas, such as choline binding site, catalytic triad, oxyanion hole, and "FGESAG" characteristic structure (Supplementary Fig. 3). The *nAChR* sequence of *H. discus hannai* is the most homologous to *Aplysia californica* (up to 68.9%), followed by *Amphibalanus amphitrite* (52.01%), but is the least homologous to *Pandalus japonicus* (only 43.31%) (Supplementary Fig. 4). The AchE of *H. discus hannai* first clusters into a small branch with Chrysomelidae *Leptinotarsa decemlineata*. It then clusters with invertebrates *Musca domestica*, *Schistosoma japonicum*, and *Meloidogyne incognita* and finally with molluscan *Physella acuta* and *Azumapecten farreri* (Supplementary Fig. 5a). The *nAChR* of *H. discus hannai* first clusters into a small branch with *Branchiostoma floridae*, suggesting that its molecular evolutionary status generally coincides with the biological taxonomic status of *P. acuta*. It then clusters with invertebrates *Pandalus japonicus*, *Crassostrea gigas*, and *Hirudo verbenae* (Supplementary Fig. 5b).

3.4. Diurnal changes and cosine analysis of Ach concentration and the expression levels of AchE and nAChR

To ascertain the diurnal change in other components of the cholinergic system, the Ach concentration was initially determined over the course of 24 h. The Ach concentration reached its maximum value at ZT12, but did not significantly differ between ZT16 and ZT20 (Fig. 3, $P > 0.05$). The expression levels of AchE exhibited a significant cosine rhythm during the day/night cycle, and peaked at ZT03:36 (Table 2, $P < 0.05$). No significant differences were identified with respect to the expression levels of *nAChR* during the day/night cycle, and the cosine analysis also suggested no rhythmicity in respect of the expression level of *nAChR* during the day/night cycle ($P > 0.05$).

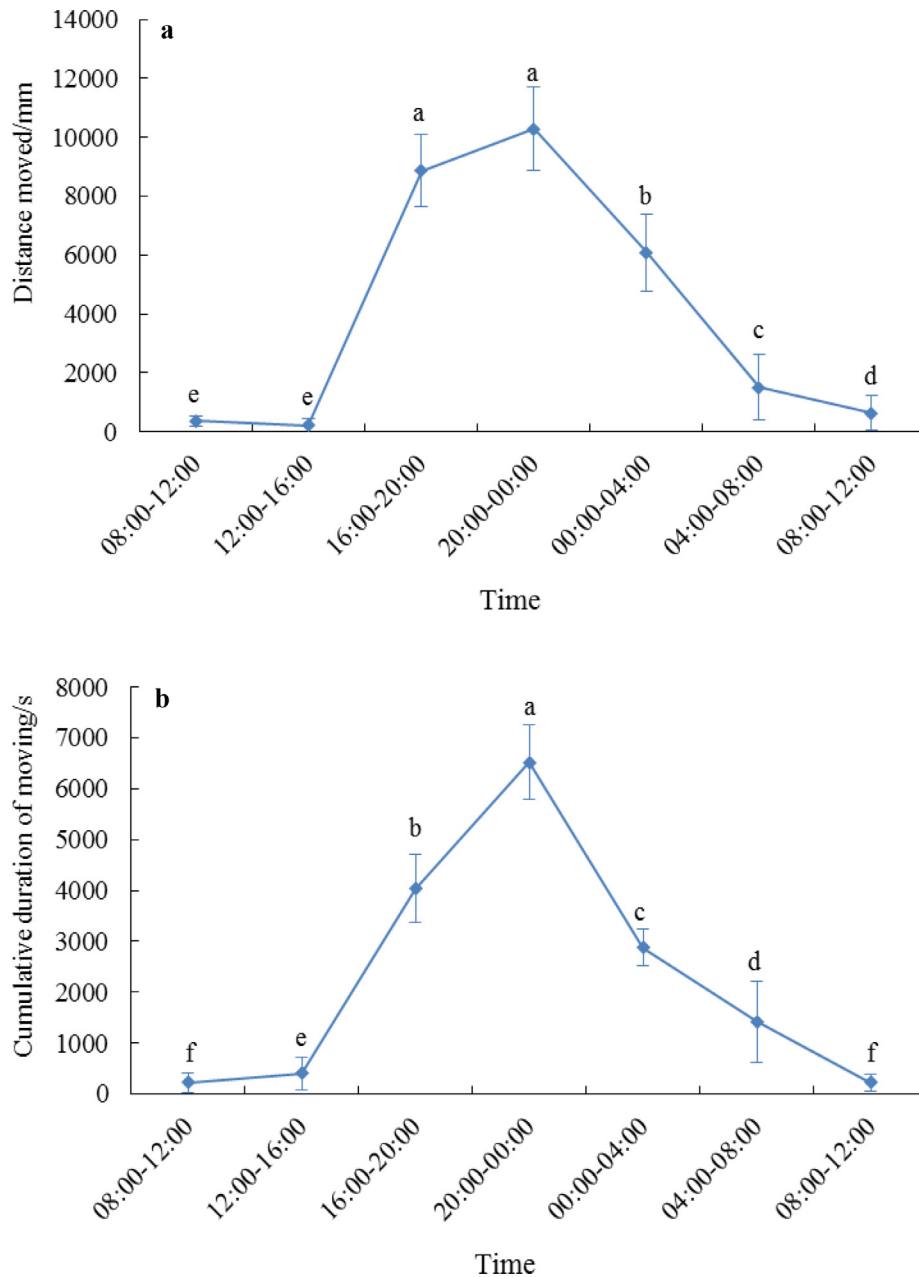


Fig. 1. Locomotory performance of *Haliotis discus hannai* at 12 light:12 dark: (a) distance moved; (b) cumulative duration of moving. Data are means and standard deviations, sample size = 32. Significant variations were found by one-way analysis of variance, $P < 0.05$, followed by Tukey test. Different letters denote significant differences between time periods.

3.5. Expression levels of *AchE*, *nAChR* in different tissues of abalone and analysis of their in situ hybridization locations

The expression levels of *AchE* in the cerebral ganglion were significantly higher than those in all other tissues (Supplementary Fig. 6, $P < 0.05$). The expression levels in the hepatopancreas were the lowest, but not significantly different from those in the intestine. The expression levels of *nAChR* were also highest in the cerebral ganglion, but not significantly different from those in the gills (Supplementary Fig. 6, $P > 0.05$). The cerebral ganglion lies above the buccal mass (Fig. 4). Compared to the negative control group, positive hybridization signals of *AchE* and *nAChR* were detected in the peripheral region of the cerebral ganglia, while almost no positive signals were detected from the medulla of the cerebral ganglia.

3.6. Effects of different inhibitor concentrations on critical components of cholinergic nervous system and movement behavior of abalones

In contrast with the control and saline groups, the expression levels of *AchE* were significantly reduced in the inhibitor neostigmine injected groups, while the content of *Ach* and the expression levels of *nAChR* increased significantly following the injection of different concentrations of the inhibitor (Supplementary Fig. 7, $P < 0.05$). However, no dose effect was found after injection of different concentrations of the inhibitor, indicating that the *Ach* content and the expression levels of *nAChR* were not significantly different from group to group. The cumulative movement distance and duration of abalones increased significantly following the injection of different concentrations of the inhibitor *AchE* (Fig. 5, $P < 0.05$). The movement distance and duration of abalones

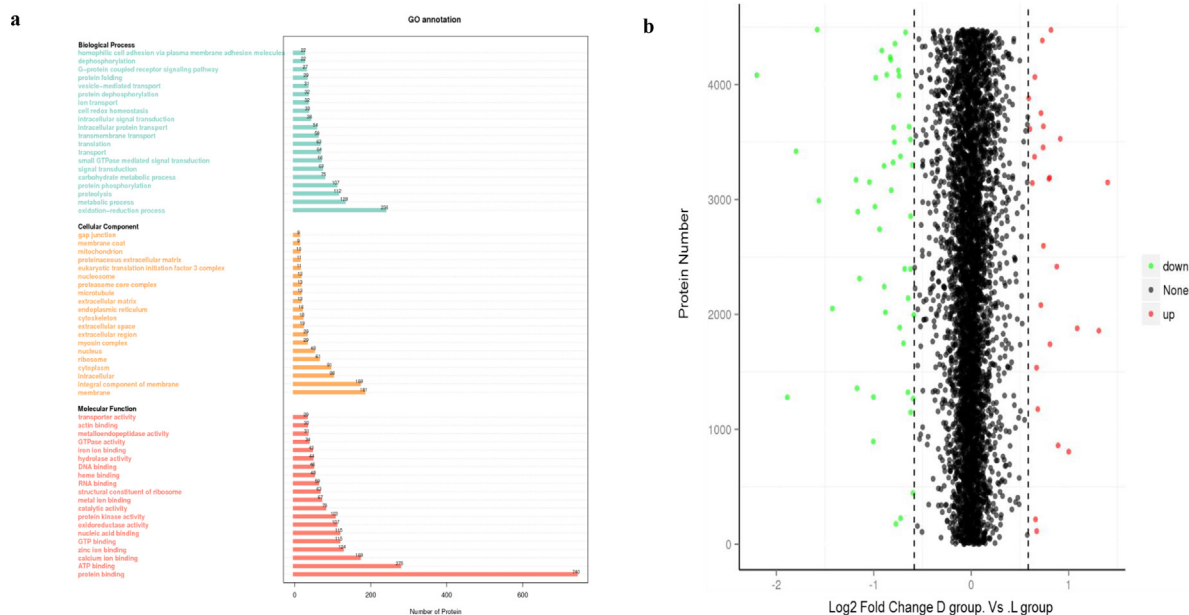


Fig. 2. Gene Ontology (GO) database annotations of the proteins discussed in this study (a). GO is categorized into: 1) Cellular Components; 2) Molecular Functions; and 3) Biological Processes. The plot shows only the top 20 results in each category. The horizontal coordinate denotes the number of proteins, and the vertical coordinate denotes the annotated GO terms. Principal component analysis in respect of the samples taken from Group D and L (b). The horizontal coordinate PC1 and the vertical coordinate PC2 represent the score of the principal component rankings in first and second place, respectively; the scatter spots in different colors indicate samples from different groups; and the oval line shows the 95% confidence interval. Cluster heat plot of the different proteins between Group D and L (c). The vertical axis denotes the clustering of samples and the horizontal axis denotes the clustering of proteins. Shorter cluster branches indicate higher similarity levels. Horizontal comparisons show the clustering relations of the content of proteins between Group D and L.

injected at a concentration of 1.50×10^{-6} mol were the longest, but not significantly different from those injected with 2.99×10^{-6} mol ($P > 0.05$). During the first hour of the experiment, the cumulative movement distance and duration of abalones injected with 2.99×10^{-6} mol were significantly longer than those in any other group ($P < 0.05$). Between 03:00–04:00, the cumulative movement distance in abalones injected with 2.99×10^{-6} mol and 1.50×10^{-6} mol were significantly greater than those in any other group. Between 03:00–04:00, the cumulative movement duration of abalones injected with 1.50×10^{-6} mol were significant longer than those in any other group ($P < 0.05$).

3.7. Diurnal changes and cosine analysis of *Bmal1* expression levels

To demonstrate whether *Bmal1*, a key biological clock gene, is directly involved in the regulation of abalone's rhythmic behavior, the expression levels of *Bmal1* over the course of 24 h were determined. The expression levels of *Bmal1* reached their maximum at ZT24, and were significantly different from those at ZT16 and ZT20 (Supplementary Fig. 8, $P < 0.05$). Cosine analysis also suggested that the expression levels of *Bmal1* exhibited significant diurnal rhythmicity, with a peak at ZT04:03 (Table 2, $P < 0.05$).

3.8. Interactions between *Bmal1* and AchE or nAChR validated by co-immunoprecipitation

HA-*Bmal1* and Flag-AchE plasmids were co-transfected into HEK 293 T cells, and the overexpressed proteins were analyzed *in vitro*. Using anti-Flag antibodies for detection, Flag-AchE was shown to be enriched in the precipitate, and the presence of the HA-*Bmal1* protein was also detected using anti-HA antibodies. The immunoprecipitation experiment results were clear, suggesting that *Bmal1* binds directly to AchE (Fig. 6a). After the HA-*Bmal1* and Flag-nAChR plasmids were co-transfected into HEK293T cells, Flag-nAChR was also detected using anti-Flag antibodies,

enriching the precipitate. The presence of the HA-*Bmal1* protein was also detected using anti-HA antibodies, suggesting that *Bmal1* can directly bind to nAChR (Fig. 6b).

3.9. Transcriptional regulatory activity of *Bmal1* in AchE and nAChR detected by dual luciferase reporter gene assay and EMSA

AchE and nAChR promoter sequences were obtained via a cloning process, in which the length of AchE promoter sequence was 2211 bp (Supplementary Fig. 9) and that of nAChR promoter sequence was 2067 bp (Supplementary Fig. 10). E'-box (CACGTT) sequence was detected at 2176–2181 upstream of the AchE gene ATG. E-box (CACGTG) sequence was detected at 151–156 and 386–391 upstream of the nAChR gene ATG, which is the essential element for *Bmal1* binding to AchE and nAChR. After pGL-AchE MT promoter reporter gene plasmid was co-transfected with pcDNA3.1 (+) empty expression plasmid (NC) and pcDNA3.1/Cg *Bmal1* expression plasmid, the relative luciferase activity in the pGL-AchE MT promoter group (mutant type, MT) was 0.370 and 0.398, respectively (Fig. 7a). After pGL-AchE WT promoter reporter gene plasmid was co-transfected with pcDNA3.1 (+) empty expression plasmid (NC) and pcDNA3.1/Cg *Bmal1* expression plasmid, the relative luciferase activity in the pGL-AchE WT promoter group (wild-type, WT) was 0.538 and 1.986, respectively. Compared with the group transfected with the empty expression plasmid pcDNA3.1 (+) (NC), the relative luciferase activity of pGL-AchE promoter in the group transfected with pcDNA3.1/Cg *Bmal1* expression plasmid was enhanced significantly ($P < 0.05$). Compared with *Bmal1* + AchE-WT, the fluorescence intensity of AchE promoter in *Bmal1* + AchE-MT was significantly reduced following the mutation of AchE promoter ($P < 0.05$), suggesting that *Bmal1* has a positive regulatory effect on AchE.

The experimental results concerning the transcriptional regulatory activity of *Bmal1* within the nAChR promoter region revealed that the relative luciferase activity of pGL-nAChR promoter in the

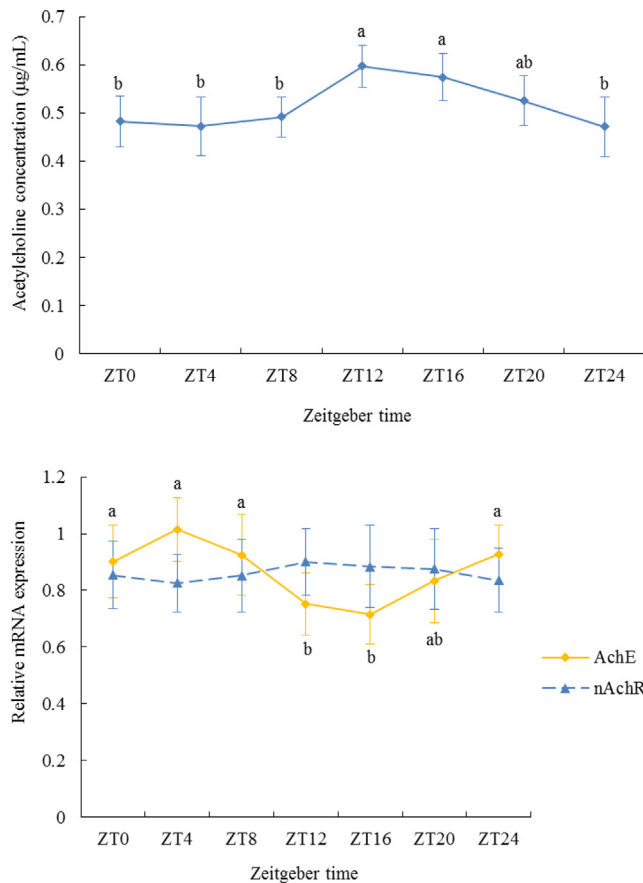


Fig. 3. Concentration of acetylcholine in the hemolymph of abalones and the expression levels of the *acetylcholinesterase* (*AchE*) and *acetylcholine receptor* (*nAChR*) in the cerebral ganglia determined during a continuous 24 h period. ZT0, ZT4, ZT8, ZT12, ZT16, ZT20, and ZT24 represent 08:00, 12:00, 16:00, 20:00, 00:00, 04:00, and 08:00, respectively. Different lowercase letters indicate significant differences in the gene expression levels between sampling times ($n = 6$, $P < 0.05$).

group transfected with pcDNA3.1/Cg *Bmal1* expression plasmid was significantly enhanced ($P < 0.05$) compared with the group transfected with empty expression plasmid pcDNA3.1 (+) (NC). Compared with *Bmal1* + *nAChR*-WT, the fluorescence intensity of *nAChR* promoter in *Bmal1* + *nAChR*-MT was significantly reduced following the mutation of *nAChR* promoter ($P < 0.05$), suggesting that *Bmal1* has positive regulatory effects on the transcription of *nAChR*.

The expression plasmid was constructed by linking *Bmal1* into the pT7CFE1-Chis Expression Vector. The HeLa cell lysate was used to express the protein *in vitro*, and the *Bmal1* recombinant protein with His tag was obtained. Then, the *Bmal1*-specific antibody was used to determine the protein size using western blotting. As a result, *Bmal1* was successfully induced and its protein size was about 50 kDa (Fig. 7b). To evaluate whether *Bmal1* can directly bind to the promoter sequences of downstream target genes *AchE* and *nAChR*, the induced *Bmal1* protein and the promoter sequences of downstream genes were used to conduct the EMSA experiment. Compared to the negative control group, there was an obvious migration band in the lane when DNA probes labeled with *AchE*, *nAChR*, and *Bmal1* protein were added at the same time, implying that *AchE* and *nAChR* promoters and *Bmal1* protein formed a covalent DNA-protein complex (Fig. 7c). However, when an excessive amount of unlabeled DNA probes (competitive probe DNA) was added to the complex, the unlabeled DNA probe competitively bound to the protein, resulting in weakening or disappearance of the migration band. The EMSA experiment showed that

Bmal1 protein can specifically bind to the promoter sequences of *AchE* and *nAChR*, suggesting that *AchE* and *nAChR* as downstream genes are directly regulated by *Bmal1*.

3.10. Effects of interference of *Bmal1* on the expression levels of *AchE* and *nAChR*

Injection doses of 0.5 µg, 1 µg, and 2 µg of *Bmal1* effectively silenced the *Bmal1* gene in the ds*Bmal1* experimental group (Fig. 8). The 2 µg injection dose resulted in the lowest expression levels of *Bmal1*. However, the expression levels of *Bmal1* did not decrease with increasing injection dose. Conversely, the expression levels of *Bmal1* did increase when the injection dose was 5 µg. Twenty-four hours after silencing the *Bmal1* gene, the expression levels of *AchE* and *nAChR* in the ds*Bmal1* group decreased significantly compared with the dsEGFP and PBS control groups (Fig. 8, $P < 0.05$).

4. Discussion

Diurnal rhythms result from various mechanisms depending on organism-specific biological clock systems and complex regulatory networks comprising clock-controlled genes. Regulated by these networks, organisms undergo rhythmic oscillations with a period of about 24 h. The forms displayed by these oscillations exhibit the rhythmic patterns of transcription and expression of core rhythmic genes in the biological clock system. The expression of downstream genes is regulated and controlled by the biological clock, and the rhythmic changes in the synthesis of certain important functional proteins, thereby regulating cyclic activity in the entire metabolic system of the organism. The maintenance of these rhythmic variations depends on the cyclic operation of the organisms' biological clock system [30,48]. We observed that abalone movement peaks from 16:00 every day to 04:00 the following day, typical for a nocturnal creature. During this period, their movement duration and distance is greatest between 20:00–00:00. Using an infra-red camera, Gao et al. (2021) found that at light cycles of 12L:12D and 24L:0D, the maximum values of the cumulative movement distance and duration of *H. discus hannai* occurred between 00:00–03:00. The results of the cosine analysis suggested that the melatonin content and expression levels of *AANAT* and *ASMT* in the 12L:12D and 24L:00 groups exhibited a significant cosine diurnal rhythm and tended to be "higher during the day and lower during the night", suggesting that abalones maintain their diurnal rhythm regardless of changes in the light cycle. Even though *H. gigantea* tends to be more shy and less active than *H. discus hannai*, the feeding behaviors of the two species show significant diurnal rhythms, with feeding peaks at ZT12 (00:00) [46], further demonstrating that light is one of the external environmental factors most likely to impact the timing of biological rhythms. In the course of the experiment, food was provided at 17:00 pm every day. This feeding method was fixed based on the fact that abalone feeding activity starts at nightfall. The feeding amount was calculated using 3% of the wet body weight of abalone. There was food residue at the end of the 24-h experiment, but we also acknowledge that feeding at ZT12 could have led to this anticipatory locomotor activity increase. The movement patterns of *Apteronomobius asahinai* show a clear diurnal rhythm, with a cycle of about 12.6 h [56]; 2017). Under similar low tide conditions, *Apteronomobius asahinai* tends to be more active during the night than the day. The use of RNAi technology reduces the expression of diurnal genes (*Period* or *Clock*), resulting in disturbances to rhythmic behaviors in constant darkness [60]; 2014). Both the brain and eyestalk ganglia have been shown to possess the molecular machinery required for the generation of a diurnal pacemaker

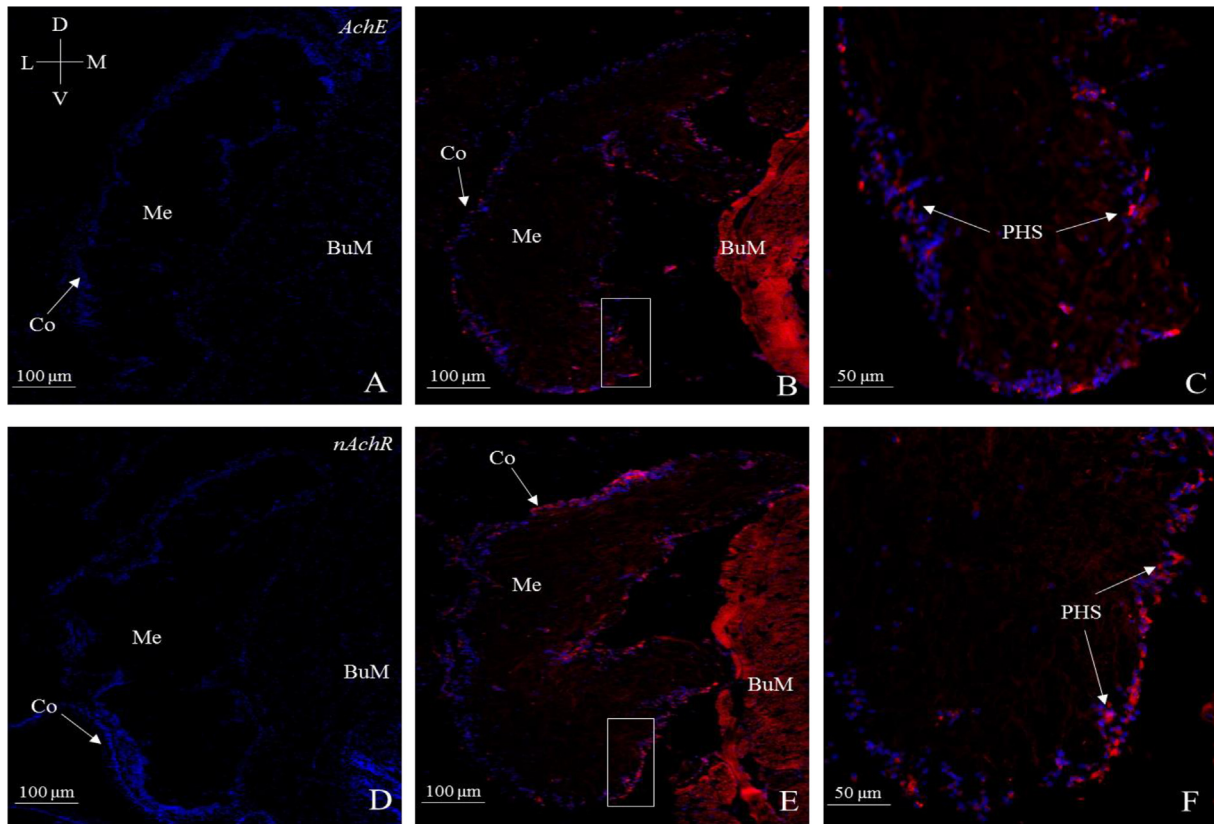


Fig. 4. Spatial expression of *AchE* and *nAChR* in the cerebral ganglion of *H. discus hannai*. Sections were dipped in DAPI staining solution. A. D. Negative control section shows no red positive signals. B. E. The boxed area shows numerous positive signals throughout the peripheral region of the ganglion. C. F. High-power micrograph of (B. E) showing red positive signals throughout the peripheral region of the ganglion (arrows). V, ventral; D, dorsal; M, medial; L, lateral; Co, cortex; Me, medulla; BuM, buccal mass; PHS, positive hybridization signals. (For interpretation of the references to color in this figure legend, the reader is referred to the web version of this article.)

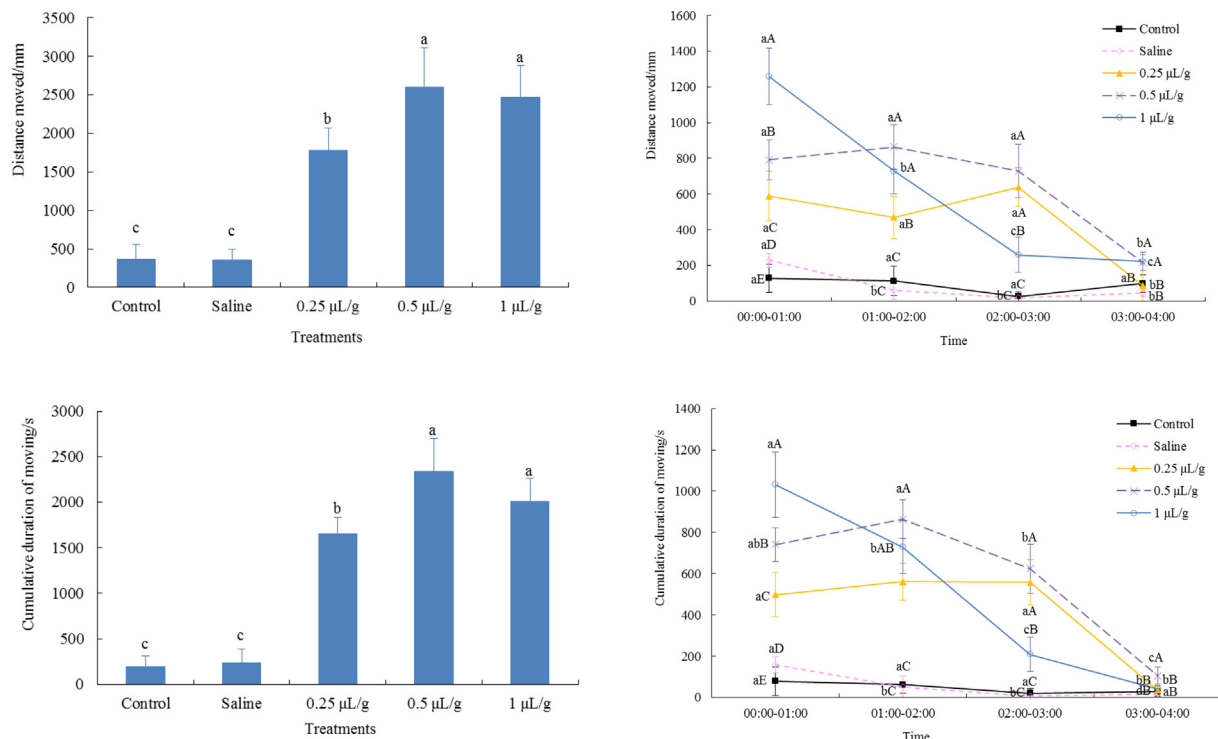


Fig. 5. Effects of injection of the *acetylcholinesterase* (*AChE*) inhibitor on the cumulative movement distance and duration of abalones during a 4 h period. Different lowercase letters indicate significant differences in the behavioral parameters of abalones at different treatments and sampling times ($n = 12, P < 0.05$). Different uppercase letters indicate significant differences in the behavioral parameters of abalones among different treatments at the same sampling time ($n = 12, P < 0.05$).

Table 2

Cosinor analysis results for Ach concentration in the hemolymph and relative expression of *AchE*, *nAChR*, and *Bmal1* genes in the cerebral abalone ganglions determined during a continuous 24-h period.

Target	Mesor	Amplitude	Acrophase	P-value
Ach	0.523456	0.0637989	ZT14:32	< 0.001
<i>AchE</i>	0.855333	0.139084	ZT03:36	< 0.001
<i>nAChR</i>	0.86337	0.0237374	ZT15:16	0.143467
<i>Bmal1</i>	0.729104	0.197553	ZT04:03	0.001

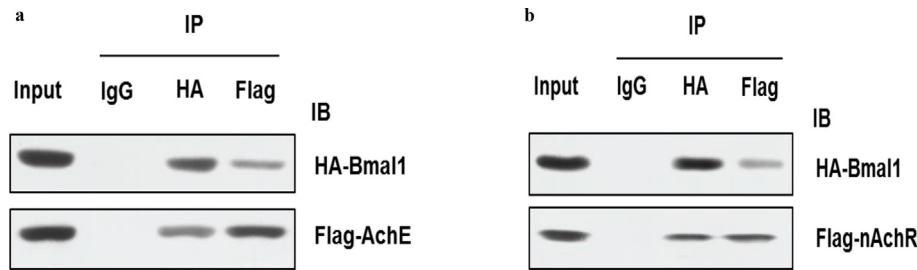


Fig. 6. Interactions were shown between *Bmal1* and acetylcholinesterase (*AchE*, a) or acetylcholine receptor (*nAChR*, b) in HEK293T cells by Co-immunoprecipitation assays. HA-*AchE* and Flag-*Bmal1* plasmids, and HA-*nAChR* and Flag-*Bmal1* plasmids were co-transfected into HEK 293 T cells, and the overexpressed proteins were analyzed *in vitro*. Cells were lysed after 48 h of transfection, centrifuged (at 500 g for 30 s), and the supernatant was then removed. 15 μ L anti-Flag-Agarose was added to the supernatant and incubated at 4 °C overnight, and then centrifuged (at 500 g for 30 s). The supernatant was discarded, 5 μ L 1 \times SDS loading buffer was added and subjected to vortex separation and denaturation, after which the target protein was detected using immunoblotting.

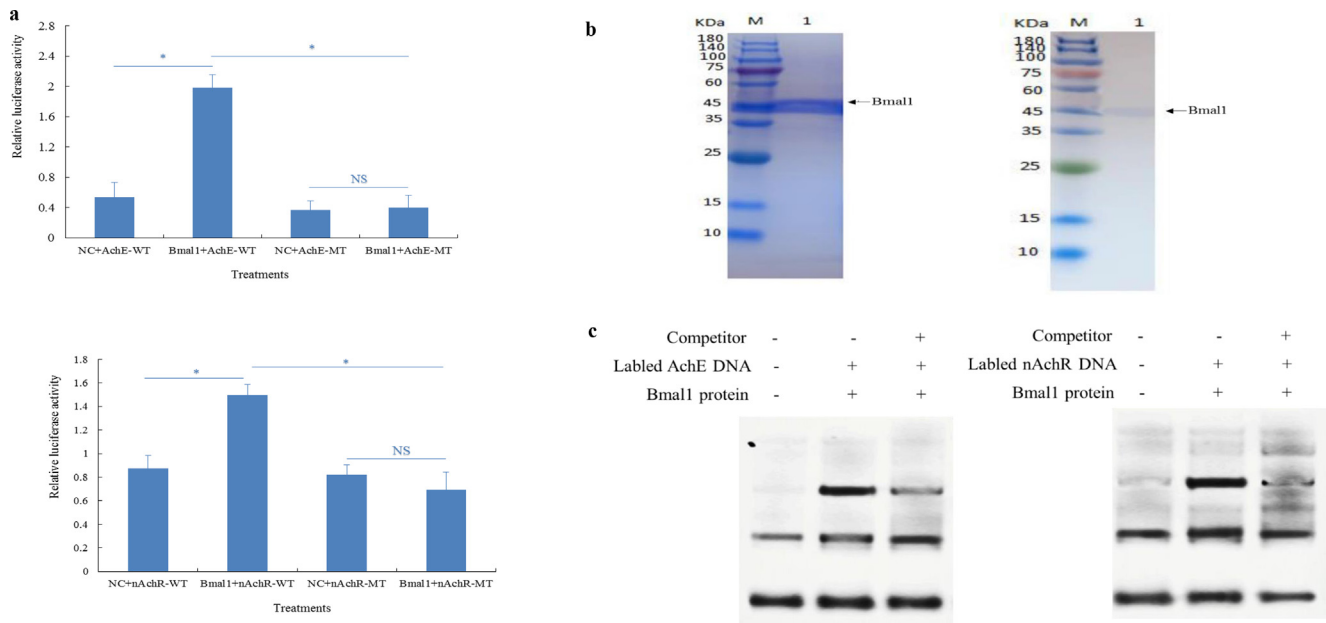


Fig. 7. (a) Dual luciferase report assay was used to analyze the transcription abilities of *Bmal1* in activation of acetylcholinesterase (*AchE*) and acetylcholine receptor (*nAChR*) in HEK 293 T cells. For the pGL3/Cg *AchE* and pGL3/Cg *nAChR* promoter groups, pGL3/Cg *AchE* promoter and pGL3/Cg *nAChR* promoter were co-transfected with pcDNA3.1 (+) (NC) and pcDNA3.1/Cg *Bmal1* in HEK293T cells, respectively. Significant difference $P < 0.05$ was labeled “***”, no significant difference $P > 0.05$ was labeled “NS”. (b) The *Bmal1* protein synthesized by *in vitro* transcription and shown by Western blot. (c) Interaction between *Bmal1* protein and the *AchE*/*nAChR* promoters.

in at least some members of the Decapoda. *Homarus americanus* CG transcriptome was generated and searched for transcripts encoding homologs of the putative brain/eyestalk ganglia diurnal signaling system proteins that were recently identified from transcriptomes specific for the lobster brain and eyestalk ganglia (Christie et al., 2018 a, b). Efforts to discover the expression patterns of diurnal clock genes and clock-controlled genes in abalone can provide evidence to understand their particular behavioral rhythms.

Proteomics can be used to study the general protein composition and activity patterns of an organism, cell, or tissue. In this

study, 75 proteins with significant differences in expression levels were identified in group D vs group L by means of TMT quantitative proteomics methodologies. *AchE* was screened three times, and its expression levels at 00:00 were significantly lower than that at 12:00 and tended to be higher during the day and lower at night. In both vertebrates and invertebrates, *AchE* is a vital neurotransmitter hydrolase that hydrolyzes ACh separation and release from ACh receptors, thereby terminating the stimulatory effect of ACh on acetylcholine receptors. This guarantees the regular conduction of nerve impulses between synapses, and maintains the normal physiological functions of the organism[39,43]. The

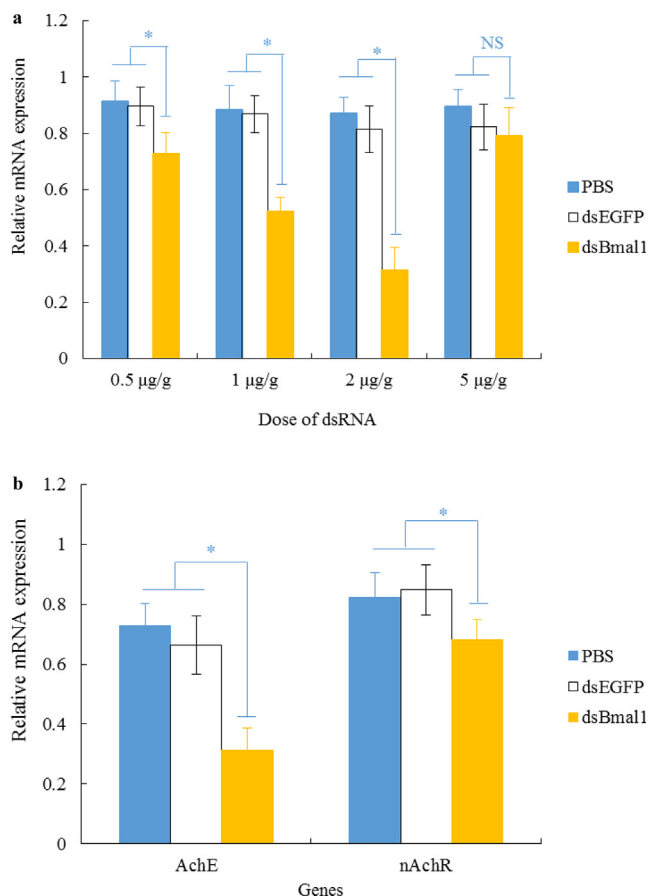


Fig. 8. (a) Silencing efficiencies of different doses of *Bmal1* dsRNA in the cerebral ganglia ($n = 5$). (b) Expression levels of *AchE* and *nAChR* in the cerebral ganglia at 24 h (h) after silencing of *Bmal1* ($n = 20$). DsEGFP stands for EGFP dsRNA injection group, dsBmal1 stands for *Bmal1* dsRNA injection group. “*” indicate significant differences ($P < 0.05$) of the gene expression levels in different treatments.

length of *AchE* varies slightly from species to species, but assessments of the full length of the gene imply that the complete encoded protein sequence is generally between 550 and 700 amino acids. For example, the gene sequence of *Drosophila melanogaster*, *Tribolium castaneum*, *Bombyx mori*, and other species encodes approximately 650 amino acids [28,44,45]. The *AchE* gene sequence has also been cloned from the optic ganglion of *Loligo opalescens* and structural analysis revealed that it also has typical conserved domains specific to *AchE*: i.e., choline binding sites, active catalytic sites, and three pairs of disulfide bonds[62]. In this study, we also noted that the expression levels of *AchE* in the cerebral ganglia of abalones were significantly higher than in any other tissue. Here, the sequence of *AChE* encoded 598 amino acids and also contained a typical carboxylesterase family domain. From continuous assays of *Ach* content, the expression levels of *AchE* and *nAChR*, and the rhythm analysis, we found that *Ach* content exhibits rhythmic changes (lower during the day and higher at night), while the expression levels of *AchE* show the reverse trend (higher during the day and lower at night). The expression levels of *nAChR* show no significant cosine rhythm, but reached a maximum value at ZT12, presenting a similar trend to the diurnal changes in *Ach* content. Therefore, we suggest that the reduction in *AchE* expression levels at night contribute to the accumulation of *Ach* in synapses, thereby ensuring the rapid transduction of nerve signals by binding to *nAChR*, as evidenced by the more active behavior of abalone during the night than the day.

Like the *nAChR* receptor in vertebrates, invertebrate *nAChR* has a variety of geometries and subunits which can be activated by

Ach. Pim van Nierop et al. [49] cloned 12 *nAChR* genes from *Lymnaea stagnalis*, whose sequence structures are highly similar to *nAChR*. Using RT-PCR and *in situ* hybridization, these receptors were found to be widely distributed in the central nervous system and peripheral neurons of *L. stagnalis*, and at least 10% of neurons were able to express *nAChR*. This study obtained similar results. The comparative study of amino acid sequence homology suggested that the *nAChR* sequence of *H. discus hannai* is highly homologous to that of other invertebrates, and that the expression levels in cerebral ganglia were higher than in other tissues. As further supported by *in situ* hybridization, *nAChR* was widely expressed in the cortex of the cerebral ganglion, but almost no positive signal was detected in the medulla. The ligand-gated ion channel is a set of transmembrane ion channel proteins which react when specific ligands, either inside or outside of the cell, bind to membrane receptors, which can be opened to allow the access of ions such as Na^+ , K^+ , Ca^{2+} , and Cl^- . When pre-synaptic neurons are excited by electrical nerve signals, neuronal cells secrete vesicles containing neurotransmitters into the synaptic cleft[64]. The neurotransmitters are then secreted into the synaptic cleft of the neuron and promptly bind to specific receptors on the cell membrane of the postsynaptic neuron. When the specific receptor of a postsynaptic neuron is a ligand-gated ion channel, conformational changes occurring after the ligand binds to the receptor will activate the ion channel, triggering ions to flow from one side of the cell membrane to the other. The transmembrane domains can form ion channel pores and the extracellular domains of the specific ligand binding sites are essential to these ligand-gated ion receptor proteins[37,7]. In this study, the domain analysis of *nAChR* revealed that *nAChR* contains two classic domains, the neurotransmitter-gated ion-channel ligand binding domain and the neurotransmitter-gated ion-channel transmembrane region, which can convert the chemical signals of the neurotransmitter into electrical signals, thereby playing a crucial part in the formation of behavioral rhythms in abalone.

In the transduction of the cholinergic nerve signal of *Caenorhabditis elegans*, any pathological change in the *ACh* signal pathway results in uncoordinated movement. The cholinergic motor neurons of the ventral nerve cord of *C. elegans* can regulate its movement by expressing *ACR-2* and *ACR-5* subunits[65,24]. Mutated *cha-1* and *unc-17* in *C. elegans* interrupt the choline signaling pathway causing signs of continuous ovulation [2]. Fabian-Fine et al. [14] have identified *Cupiennius salei* genes that encode enzymes essential for cholinergic transmission, which included choline *ACh* transferase (*ChAT*) and vesicular *ACh* transporter (*VACHT*). They used *in-situ* hybridization with an mRNA probe for *C. salei* *ChAT* gene to locate somata of cholinergic neurons in the central nervous system and immunohistochemistry with antisera against *ChAT* and *VACHT* to locate these proteins in cholinergic neurons. All three markers were similarly labeled as mostly small neurons, plus a few mid-sized neurons, in most ganglia. Some evidence has previously shown that many large neurons in the subesophageal ganglia are immunoreactive to glutamate and/or GABA, and that both transmitters were also present in axon terminals innervating the leg muscle [15]. For the desert locust *Schistocerca gregaria*, cholinergic transmission from antennal sensillae to olfactory or mechanosensory centers in the brain requires that choline acetyltransferase and the *VACHT* already be present in sensory cells in the first instar[13]. The sensory and motor functions of arthropods also depend on the activation of the choline signaling pathway. In *Omocestus viridulus*, friction caused by wing movements triggers the activation of cholinergic neurons in the archicerebrum and the pharyngeal nerve center [29,63]. Imidacloprid can specifically bind to *nAChR*, and low-dose imidacloprid can rapidly enhance the movement ability of *Apis mellifera* [42,20]. Rima et al. (2020) have demonstrated that cholinergic genes (*AchE*,

nAChR, and vesicular acetylcholine transporters) are initially expressed in the zebrafish embryonic spinal cord. Their dynamical downregulation during development suggests that cholinergic signaling may play a pivotal role during the formation of intraspinal locomotor circuit. In *Mytilus edulis*, ACh can regulate the heartbeat and the movement of the gill cilia (Burbrink et al., 1953; [23]. In *Katelsia rhytiphora* and *K. scalarina*, ACh can affect the movement of the rectal muscles and have an impact their digestive functions [22]. Neostigmine methylsulfate is often used to treat severe and urgent myasthenia gravis and postoperative abdominal bloating, and can suppress the activity of AchE to stimulate the entire cholinergic effect, and also directly stimulate the nicotinic N2 receptors on the motor endplates of skeletal muscles (Cridge Harry et al., 2021). After using neostigmine methylsulfate as an inhibitor, the expression levels of AchE at three experimental concentrations significantly reduced cholinesterase activity, while the Ach content and expression levels of nAChR rose significantly, suggesting that neostigmine methylsulfate can effectively reduce the expression levels of AchE. After neostigmine methylsulfate injection, the cumulative movement distance and duration of abalones increased significantly, especially within the first hour after injection. The movement distance and duration of abalones in all of the groups injected with the various concentrations of neostigmine methylsulfate were significantly higher than in the control group, which further suggests that the movement behavior of abalone is governed by the cholinergic nervous system. The rhythmic expression of key clock genes and proteins in cells produces rhythmic signals in an organism, and the activation and spatiotemporal regulation of these key clock genes is induced by the Clock/Bmal1 heterodimer, as suggested by their rhythmic physiological and behavioral expression patterns [26]. Prolonged feeding of a high-fat diet causes abnormal liver mitochondrial function in Bmal1 liver-specific knockout mice, resulting in lower insulin sensitivity (Jacobi et al. 2015). In the white fat of Bmal1 knockout mice, the expression levels of adipose triglyceride lipase and hormone-sensitive lipase immediately cause a loss in rhythmicity, suggesting that the rhythm of lipid synthesis and metabolism is regulated by Bmal1 (Fontaine et al., 2003). In this study, the expression levels of Bmal1 exhibited a cosine rhythm. Dual luciferase reporter gene detection revealed that *Bmal1* can bind to the promoters of *AchE* and *nAChR*, suggesting that *Bmal1* mediates the cholinergic system by combining with *AchE* and *nAChR*, thereby directly effecting the regulation of diurnal rhythm in abalone. Due to the specificity of the species, no suitable antibody is currently available. In the future, an antibody will be necessary to demonstrate the role of the Bmal1-mediated cholinergic system in regulating the rhythm behavior of abalone *in vivo* experiments.

Following the determination of the concentration of Ach and the expression levels of *AchE* and *nAChR*, and the analysis of the diurnal cosine rhythm of the key components of the cholinergic system, it was noted that the concentration of Ach rose and the expression level of AchE fell during the peak movement period of abalones, which in turn helps Ach to maintain its stimulatory effects on nAChR, thus ensuring the regular transduction of nerve impulses. Four hours after the injection of different concentrations of neostigmine methylsulfate as an AchE inhibitor, the Ach concentration and expression levels of nAChR rose significantly, and the abalones in the injected groups tended to be more active than those in the control and normal saline injected groups, suggesting that the cholinergic system plays a regulatory role in maintaining the rhythmic behavior of abalone. *Bmal1*, as a core diurnal clock gene, not only exhibits a cosine rhythm with respect to its expression levels by day and night, but also binds to the E-box regions of the *AchE* and *nAChR* promoters to initiate the course of gene transcription. The stable operation of the cholinergic system is critical to maintaining the normal physiological functions of abalone,

Bmal1 is involved in the regulatory process of the behavioral rhythm of abalone by mediating the rhythmic expression of key components of the cholinergic system. A stable behavioral rhythm not only results from the prolonged adaptation of abalone to cyclical changes in the external light environment, but also provides a reference for identifying its adaptive life history strategy and for protecting and increasing populations of bottom dwelling species of economic importance.

Data availability

All data generated or analysed during this study are included in this published article. The mass spectrometry proteomics data have been deposited to the ProteomeXchange Consortium via the PRIDE partner repository with the dataset identifier PXD029815.

Declaration of Competing Interest

The authors declare that they have no known competing financial interests or personal relationships that could have appeared to influence the work reported in this paper.

Acknowledgements

We would like to thank Chengyun Li and Jianxiong Li for their assistance with abalone collection and rearing. We appreciate the very helpful and constructive comments and suggestions from Prof. Luoying Zhang and Guang Li for improving the manuscript. This research was supported by grants from the National Key Research and Development Program of China [2018YFD0901400]; Key S & T Program of Fujian Province (No. 2020NZ08003); China Agriculture Research System of MOF and MARA; China Postdoctoral Science Foundation Grant [2019 M650153, 2021 T140393]; and the Outstanding Postdoctoral Scholarship from the State Key Laboratory of Marine Environmental Science at Xiamen University. We are also grateful for the support from the Germplasm resource-sharing platform of aquatic species in Fujian Province and XMU-MRB abalone research center.

Appendix A. Supplementary data

Supplementary data to this article can be found online at <https://doi.org/10.1016/j.csbj.2022.05.038>.

References

- [1] Ahmed NY, Knowles R, Dehorter N. New insights into cholinergic neuron diversity. *Front Mol Neurosci* 2019;12:204. <https://doi.org/10.3389/fnmol.2019.00204>.
- [2] Bany IA, Dong MQ, Koelle MR. Genetic and cellular basis for acetylcholine inhibition of *Caenorhabditis elegans* egg-laying behavior. *J Neurosci* 2003;23:8060–9. [https://doi.org/10.1016/S0304-3940\(03\)00712-2](https://doi.org/10.1016/S0304-3940(03)00712-2).
- [3] Bass J, Takahashi JS. Circadian integration of metabolism and energetics. *Science* 2010;330:1349–54. <https://doi.org/10.1126/science.1195027>.
- [5] Boppana S, Kendall N, Akininsola O, White D, Patel K, Lawal H. Immunolocalization of the vesicular acetylcholine transporter in larval and adult *Drosophila* neurons. *Neurosci Lett* 2017;643:76–83. <https://doi.org/10.1016/j.neulet.2017.02.012>.
- [7] Cascio M. Structure and function of the glycine receptor and related nicotinic receptors. *J Biol Chem* 2004;279:19383–6. <https://doi.org/10.1074/jbc.R300035200>.
- [12] Deshpande S, Freyberg Z, Lawal HO, Krantz DE. Vesicular neurotransmitter transporters in *Drosophila melanogaster*. *BBA Biomembranes* 2020;1862:.. <https://doi.org/10.1016/j.bbamem.2020.183308>183308.
- [13] Ehrhardt E, Boyan G. Evidence for the cholinergic markers ChAT and vAChT in sensory cells of the developing antennal nervous system of the desert locust *Schistocerca gregaria*. *Invert Neurosci* 2020;20:19. <https://doi.org/10.1007/s10158-020-00252-4>.
- [14] Fabian-Fine R, Anderson CM, Roush MA, Johnson JAG, Liu H, French AS, et al. The distribution of cholinergic neurons and their co-localization with FMRFamide, in central and peripheral neurons of the spider *Cupiennius*

- salei*. Cell Tissue Res 2017;370:71–88. <https://doi.org/10.1007/s00441-017-2652-6>.
- [15] Fabian-Fine R, Meisner S, Torkkeli PH, Meinertzhagen IA. Colocalization of γ -aminobutyric acid and glutamate in neurons of the spider central nervous system. Cell Tissue Res 2015;362:461–79. <https://doi.org/10.1007/s00441-015-2241-5>.
- [16] French AS, Li AW, Meisner S, Torkkeli PH. Upstream open reading frames and Kozak regions of assembled transcriptome sequences from the spider *Cupiennius salei*. Selection or chance? Gene 2014;539:203–8. <https://doi.org/10.1016/j.gene.2014.01.079>.
- [17] Gao X, Luo X, You W, Ke C. Circadian movement behaviours and metabolism differences of the Pacific abalone *Haliotis discus hanna*. J Photoch Photobio B 2020;211:1–7. <https://doi.org/10.1016/j.jphotobiol.2020.11.1994>.
- [18] Gauthier M, Dacher M, Thany SH, Niggebrügge C, Déglise P, Klujevic P, et al. Involvement of α -bungarotoxin-sensitive nicotinic receptors in long-term memory formation in the honeybee (*Apis mellifera*). Neurobiol Learn Mem 2006;86:164–74. <https://doi.org/10.1016/j.nlm.2006.02.003>.
- [19] Gekakis N, Staknis D, Nguyen HB, Davis FC, Wilsbacher LD, King DP, et al. Role of the clock protein in the mammalian circadian mechanism. Science 1998;280:1564–9. <https://doi.org/10.1126/science.280.5369.1564>.
- [20] Greenberg MJ. Species specific effect of acetylcholine on bivalve reclus. Science 1966;154:1015–7. <https://doi.org/10.1126/science.154.3752.1015>.
- [21] Greenberg MJ. A comparison of acetylcholine structure-activity relations on the hearts of bivalve molluscs. Comp Biochem Physiol 1970;33:259–94. [https://doi.org/10.1016/0010-406X\(70\)90349-X](https://doi.org/10.1016/0010-406X(70)90349-X).
- [22] Hallam S, Singer E, Waring D, Jin Y. The *C. elegans* NeuroD homolog *cnd-1* functions in multiple aspects of motor neuron fate specification. Development 2000;127:4239–52. <https://doi.org/10.1007/s004290000119>.
- [23] Han DH, Lee YJ, Kim K, Kim CJ, Cho S. Modulation of glucocorticoid receptor induction properties by core circadian clock proteins. Mol Cell Endocrinol 2014;383:170–80. <https://doi.org/10.1016/j.mce.2013.12.013>.
- [24] Hansen KF, Sakamoto K, Obrietan K. MicroRNAs: a potential interface between the circadian clock and human health. Genome Med 2011;3:10. <https://doi.org/10.1186/gm224>.
- [25] Hao H, Allen DL, Hardin PE. A circadian enhancer mediates PER-dependent mRNA cycling in *Drosophila melanogaster*. Mol Cell Biol 1997;17:3687–93. <https://doi.org/10.1073/pnas.95.10.5474>.
- [26] Harel M, Kryger G, Rosenberry TL, Mallender WD, Lewis T, Fletcher RJ, et al. Three-dimensional structures of *Drosophila melanogaster* acetylcholinesterase and of its complexes with two potent inhibitors. Protein Sci 2000;9:1063–72. <https://doi.org/10.1110/ps.9.6.1063>.
- [27] Heinrich R, Hedwig B, Elsner N. Cholinergic activation of stridulatory behaviour in the grasshopper *Omocestus viridulus* (L.). J Exp Biol 1997;200:1327–37. <https://doi.org/10.1242/jeb.200.9.1327>.
- [28] Herzog ED. Neurons and networks in daily rhythms. Nat Rev Neurosci 2007;8:790–802. <https://doi.org/10.1038/nrn2215>.
- [29] Hogenesch JB, Gu YZ, Jain S, Bradfield CA. The basic-helix-loop-helix-PAS orphan MOP3 forms transcriptionally active complexes with circadian and hypoxia factors. Proc Natl Acad Sci USA 1998;95:5474–9. <https://doi.org/10.1073/pnas.95.10.5474>.
- [30] Hoogerwerf WA, Hellmich HL, Cornéliussen G, Halberg F, Shahinian VB, Bostwick J, et al. Clock gene expression in the murine gastrointestinal tract: endogenous rhythmicity and effects of a feeding regimen. Gastroenterology 2007;133:1250–60. <https://doi.org/10.1053/j.gastro.2007.07.009>.
- [31] Hosoda H, Kida S. NSP-C contributes to the upregulation of CLOCK/BMAL1-mediated transcription. Cytotechnology 2019;71:453–60. <https://doi.org/10.1007/s10616-018-0266-9>.
- [32] Jaiteh M, Taly A, Héhin J. Evolution of pentameric ligand-gated ion channels: Pro-loop receptors. PLoS ONE 2016;11:1–11. <https://doi.org/10.1371/journal.pone.0151934>.
- [33] Kim JI, Jung CS, Koh YH, Lee SH. Molecular, biochemical and histochemical characterization of two acetylcholinesterase cDNAs from the German cockroach *Blattella germanica*. Insect Mol Biol 2006;15:513–22. <https://doi.org/10.1111/j.1365-2583.2006.00666.x>.
- [34] Kim TW, Jeong JH, Hong SC. The impact of sleep and circadian disturbance on hormones and metabolism. Int J Endocrinol 2015;2015:1–11. <https://doi.org/10.1155/2015/591729>.
- [35] Kumar S, Chen D, Jang C, Nall A, Zheng XZ, Sehgal A. An ecdysone-responsive nuclear receptor regulates circadian rhythms in *Drosophila*. Nat Commun 2014;5:5697. <https://doi.org/10.1038/ncomms6697>.
- [36] Lambin M, Armengaud C, Raymond S, Gauthier M. Imidacloprid-induced facilitation of the proboscis extension reflex habituation in the honeybee. Arch Insect Biochem 2001;48:129–34. <https://doi.org/10.1002/arch.1065>.
- [37] Lee DW, Kim SS, Shin SW, Kim WT, Boo KS. Molecular characterization of two acetylcholinesterase genes from the oriental tobacco budworm, *Helicoverpa assulta* (Guenée). BBA-Gen Subjects 2006;1760:125–33. <https://doi.org/10.1016/j.bbagen.2005.10.009>.
- [38] Li B, Wang Y, Liu H, Xu Y, Wei Z, Chen Y, et al. Genotyping of acetylcholinesterase in insects. Pestic Biochem Phys 2010;98:19–25. <https://doi.org/10.1016/j.pestbp.2010.04.004>.
- [39] Lu Y, Pang Y, Park Y, Gao X, Yao J, Zhang X, et al. Genome organization, phylogenies, expression patterns, and three-dimensional protein models of two acetylcholinesterase genes from the red flour beetle. PLoS ONE 2012;7:1–7. <https://doi.org/10.1371/journal.pone.0032288>.
- [40] Lyu M, Gao X, Zhang M, Lin S, Luo X, You W, et al. Comparative study of the feeding characteristics and digestion physiology of *Haliotis discus hanna* and *Haliotis gigantean*. Front Mar Sci 2021;8:1–11. <https://doi.org/10.3389/fmars.2021.751401>.
- [41] Meng X, Li C, Xiu C, Zhang J, Li J, Huang L, et al. Identification and biochemical properties of two new acetylcholinesterases in the pond wolf spider (*Pardosa pseudoannulata*). PLoS ONE 2016;11:1–11. <https://doi.org/10.1371/journal.pone.0158011>.
- [42] Nakamura W, Yamazaki S, Nakamura TJ, Shirakawa T, Block GD, Takumi T. In vivo monitoring of circadian timing in freely moving mice. Curr Biol 2008;18:381–5. <https://doi.org/10.1016/j.cub.2008.02.024>.
- [43] Nierop PV, Bertrand S, Munno DW, Gouwenberg Y, Minnen JV, Spafford JD, et al. Identification and functional expression of a family of nicotinic acetylcholine receptor subunits in the central nervous system of the mollusc *Lymnaea stagnalis*. J Biol Chem 2006;281:1680–91. <https://doi.org/10.1074/jbc.M508571200>.
- [44] Panda S, Hogenesch JB, Kay SA. Circadian rhythms from flies to human. Nature 2002;417:329–35. <https://doi.org/10.1038/417329a>.
- [45] Pogenberg V, Ogmundsdóttir MH, Bergsteinsdóttir K, Schepsky A, Phung B, Deineko V, et al. Restricted leucine zipper dimerization and specificity of DNA recognition of the melanocyte master regulator MITF. Genes Dev 2012;26:2647–58. <https://doi.org/10.1101/gad.198192.112>.
- [46] Sahar S, Sassone-Corsi P. Regulation of metabolism: the circadian clock dictates the time. Trends Endocrin Met 2012;23:1–8. <https://doi.org/10.1016/j.tem.2011.10.005>.
- [47] Satoh A, Yoshioka E, Numata H. Circatidal activity rhythm in the mangrove cricket *Apteronomobius asahinae*. Biol Lett 2008;4:233–6. <https://doi.org/10.1098/rsbl.2007.0166>.
- [48] Showell SS, Martinez Y, Gondolfo S, Boppina S, Lawal HO. Overexpression of the vesicular acetylcholine transporter disrupts cognitive performance and causes age-dependent locomotion decline in *Drosophila*. Mol Cell Neurosci 2020;105:1–11. <https://doi.org/10.1016/j.mcn.2020.103483>.
- [49] Takekata H, Matsuura Y, Goto SG, Satoh A, Numata H. RNAi of the circadian clock gene *period* disrupts the circadian rhythm but not the circatidal rhythm in the mangrove cricket. Biol Lett 2012;8:488–91. <https://doi.org/10.1098/rsbl.2012.0079>.
- [50] Tulesa V, Grauso M, Arpagaus M, Giovannini E, Romani R, Rosi G. Molecular cloning and expression of a full-length cDNA encoding acetylcholinesterase in optic lobes of the squid *Loligo opalescens*: A new member of the cholinesterase family resistant to diisopropyl fluorophosphate. J Neurochem 1999;72:1250–8. <https://doi.org/10.1046/j.1471-4159.1999.0721250.x>.
- [51] Wenzel B, Hedwig B. Neurochemical control of cricket stridulation revealed by pharmacological microinjections into the brain. J Exp Biol 1999;202:2203–16. <https://doi.org/10.1242/jeb.202.16.2203>.
- [52] Williamson SM, Walsh TK, Wolstenholme AJ. The cys-loop ligand-gated ion channel gene family of *Brugia malayi* and *Trichinella spiralis*: a comparison with *Caenorhabditis elegans*. Invertebr Neurosci 2007;7:219–26. <https://doi.org/10.1007/s10158-007-0056-0>.
- [53] Winnier AR, Meir JY, Ross JM, Tavernarakis N, Driscoll M, Ishihara T, et al. UNC-4/UNC-37-dependent repression of motor neuron-specific genes controls synaptic choice in *Caenorhabditis elegans*. Gene Dev 1999;13:2774–86. <https://doi.org/10.1101/gad.13.21.2774>.

Further reading

- [4] Bookout AL et al. FGF21 regulates metabolism and circadian behavior by acting on the nervous system. Nat Med 2013;19:1147–54. <https://doi.org/10.1038/nm.3249>.
- [6] Bürbring E, Burn JH, Shelley HJ. Acetylcholine and ciliary movement in the gill plates of *Mytilus edulis*. P Roy Soc Lond B Bio 1953;141:445–66. <https://doi.org/10.1098/rspb.1953.0053>.
- [8] Christie AE et al. Circadian signaling in *Homarus americanus*: Region-specific de novo assembled transcriptomes show that both the brain and eyestalk ganglia possess the molecular components of a putative clock system. Mar Genomics 2018;40:25–44. <https://doi.org/10.1016/j.margen.2018.03.002>.
- [9] Christie AE, Yu A, Pascual MG. Circadian signaling in the northern krill *Meganctiphanes norvegica*: prediction of the protein components of a putative clock system using a publicly accessible transcriptome. Mar Genomics 2018;37:97–113. <https://doi.org/10.1016/j.margen.2017.09.001>.
- [10] Cridge H, Little A, José-López R, Pancotto T, Michaels JR, Menchetti M, et al. The clinical utility of neostigmine administration in the diagnosis of acquired myasthenia gravis. J Vet Emerg Crit Care 2021;31:647–55. <https://doi.org/10.1111/vec.13097>.
- [11] Dauchy RT et al. The influence of red light exposure at night on circadian metabolism and physiology in Sprague-Dawley rats. J Am Assoc Lab Anim 2015;54:40–50.
- [16] Fontaine C et al. The orphan nuclear receptor Rev-erb α is a peroxisome proliferator-activated receptor (PPAR) γ target gene and promotes PPAR γ -induced adipocyte differentiation. J Biol Chem 2003;278:37672–80. <https://doi.org/10.1074/jbc.M304664200>.
- [17] Food and Agriculture Organization of the United Nations (FAO), Rome, 2019. FishStatJ. www.fao.org/fishery/statistics/en.
- [34] Huang D, Sherman BT, Lempicki RA. Bioinformatics enrichment tools: paths toward the comprehensive functional analysis of large gene lists. Nucleic Acids Res 2009;37:1–13. <https://doi.org/10.1093/nar/gkn923>.

- [35] Ito C, Tomioka K. Heterogeneity of the peripheral circadian systems in *Drosophila melanogaster*: a review. *Front Physiol* 2016;7:8. <https://doi.org/10.3389/fphys.2016.00008>.
- [36] Jacobi D et al. Hepatic *bmal1* regulates rhythmic mitochondrial dynamics and promotes metabolic fitness. *Cell Metab* 2015;22:709–20. <https://doi.org/10.1016/j.cmet.2015.08.006>.
- [37] Jones P et al. InterProScan 5: genome-scale protein function classification. *Bioinformatics* 2014;30:1236–40. <https://doi.org/10.1093/bioinformatics/btu031>.
- [38] Reppert SM, Weaver DR. Coordination of circadian timing in mammals. *Nature* 2002;418:935–41. <https://doi.org/10.1038/nature00965>.
- [39] Rima M et al. Dynamic regulation of the cholinergic system in the spinal central nervous system. *Sci Rep* 2020;10:15338. <https://doi.org/10.1038/s41598-020-72524-3>.
- [40] Santos SC et al. Expression and subcellular localization of a novel nuclear acetylcholinesterase protein. *J Biol Chem* 2007;282:25597–603. <https://doi.org/10.1074/jbc.M700569200>.
- [41] Satoh A. Constant light disrupts the circadian but not the circatidal rhythm in mangrove crickets. *Biol Rhythm Res* 2017;48:459–63. <https://doi.org/10.1080/09291016.2016.1275392>.
- [42] Sethuramanujam S et al. Rapid multi-directed cholinergic transmission in the central nervous system. *Nat Commun* 2021;12:1374. <https://doi.org/10.1038/s41467-021-21680-9>.
- [43] Takekata H, Numata H, Shiga S, Goto SG. Silencing the circadian clock gene *Clock* using RNAi reveals dissociation of the circatidal clock from the circadian clock in the mangrove cricket. *J Insect Physiol* 2014;68:16–22. <https://doi.org/10.1016/j.jinsphys.2014.06.012>.